The prediction of moisture and temperature distribution in a concrete reactor containment

Åhs, Magnus; Poyet, Stéphane

2015

Document Version:
Peer reviewed version (aka post-print)

LUND FACULTY OF ENGINEERING
LUND UNIVERSITY
Division of Building Materials

The prediction of moisture and temperature distribution in a concrete reactor containment

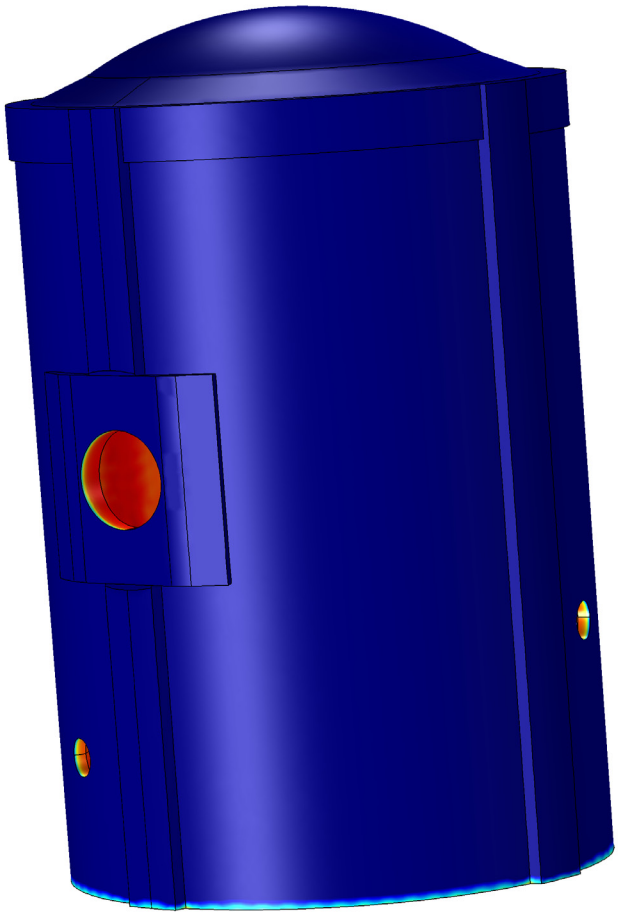

TVBM-7218 Lund 2015

The prediction of moisture and temperature distribution in a concrete reactor containment

Magnus Åhs, Stéphane Poyet

LUND UNIVERSITY

ISRN LUTVDG/TVBM—15/7218—SE(1-72)
ISSN 0348-7911 TVBM

Magnus Åhs
Lund University
Division of Building Materials
P.O. Box 118
SE-221 00 Lund
SWEDEN

Stéphane Poyet
CEA Saclay
DEN/DANS/DPC/SECR
Laboratoire d'Etude du
Comportement des Bétons
et des Argiles
Bâtiment 158, PC 25
F-91191 Gif sur Yvette
FRANCE

Preface

In the project ”Nulife-ACCEPPT”, funded by some of the nuclear power industries in France, Finland and Sweden, there was a need to make an early supply of moisture profiles of containment walls to the sub-project G3. This report is a description of the work performed in sub-project G4 Determination of current and future conditions of moisture and temperature in the structure in Work Package 2 Pre-stressed concrete containments. The report describes such an early estimation and also a later performed prediction of the reactor containment in a 3D model.

Magnus Åhs

Lund in April 2015

Summary

The objective in this research has been to predict the current and future moisture and temperature distribution in a concrete reactor containment, RC. The overall objective in this project was to create a model to be able to predict the moisture and temperature distribution in the concrete wall of the RC of a Pressurized Water Reactor, PWR. In addition, one objective was to design a model to simulate the climate exposure through an operational time of about 60 years. In order to accomplish this, the material properties to be used in a transient moisture and heat transfer model had to be estimated.

A three dimensional finite element model was developed to simulate the moisture and temperature conditions during the first 30 years of operation and also to predict the coming 30 years of an RC. The model uses the relative humidity as the driving potential. The model also presents methods to take into account the temperature dependency of the moisture properties, such as the moisture fixation i.e. sorption isotherm and the moisture transport properties, i.e. the diffusion coefficient. Thermal properties were considered to be constant, .i.e. they were assumed not to be affected by the moisture content.

The developed hygro-thermal model was applied in COMSOL Multiphysics, a mathematical software, and used in a number of simulations. The model is developed to predict moisture and temperature distributions in a RC when there is a significant temperature gradient through the concrete structure, which is the case in a PWR. The exterior surface of the RC is exposed to the natural climate.

The results from the simulated moisture distributions of a concrete RC were compared with results from measurement performed on a Swedish concrete RC, Ringhals. The simulated moisture distributions in this project and the moisture distribution determined on the Swedish concrete RC were found to qualitatively correspond to each other. There was no possibility to compare the moisture distribution quantitatively.

List of Contents

1 Introduction

In the project ”Nulife-ACCEPPT” the sub-project G4 concentrates on predicting the moisture conditions in the reactor containment walls and dome of a pressurized water reactor, PWR. The sub-project G4 is a co-operation between Lund University in Sweden and CEA in France.

1.1 Required information and tools

In order to perform a realistic prediction of the moisture conditions in the reactor containment wall there is a need to have a detailed knowledge of a number of parameters. These are listed below. In this project the available information was scarce. Therefore many of the parameters were estimated by using different methods.

1. Design properties such as geometry and material properties
    a. Detailed description of reactor containment including dimensions, liner structure, concrete type and quality, concrete mix, properties, cement type, aggregate type, etc.

A 3D geometry was delivered from KTH. The concrete mix was available.

2. Boundary conditions
    a. Current climatic conditions inside and outside of the reactor containment
        i. The climatic conditions on the both sides of the Reactor Containment, RC, walls have to be known in order to perform a realistic prediction of the concrete moisture conditions. The data should include the outside climate (temperature, relative humidity, rain, sun, surface temperature and surface relative humidity) and inside temperature (at some levels). Since there is a steel plate, impermeable to moisture transport, on the interior surface there is no need for determining the interior humidity.
        ii. Interesting information of the climate could be the variation of the surface temperature and relative humidity at different points on the exterior of the reactor containment. And this could be performed by means of non-destructive tests performed 2-4 times during the year.
    b. Temperature conditions during the past
        i. The utility’s own interior temperature surveillance measurements, if there is any, can be used to identify areas which represent the average climate and to avoid heat spots.

c. Models which describes the boundary conditions will be developed by means of the above-mentioned measurements and data

There were no recorded data available of climatic conditions neither on the outside nor on the inside of the RC. It was not possible to install measurement equipment on the site during this project, because of the restrictions to install such an equipment the RC.

3. Material properties

   a. The decisive material properties for the moisture transport analysis are desorption isotherms, moisture transport coefficients and the chemically bound water to the cement.

   b. The above-mentioned properties shall be measured on the same concrete as the reactor containment is constructed with. For example, there could be some pieces left over from earlier repairs or core-drilling, etc.

   c. If there are no pieces left over the properties shall be measured on specimens made by concrete, which has the same mix proportion and constituents as the concrete used in the reactor containment. Additionally, the properties will be estimated by available material models.

No samples of concrete from the actual RC wall were available. All concrete properties were estimated based on the available information. One set of material properties was determined by using a replica concrete cast and treated under laboratory conditions. The concrete was made from materials that are available today.

4. Computational models

   a. Models for temperature distributions and temperature variations are highly traditional, but must include accurate descriptions of the boundary conditions under paragraph 2.

   b. Models of the moisture distribution and humidity variations will include chemically bound water at early age, mostly to define the initial conditions, accurate description of the moisture and temperature gradients and the effect of the temperature level on material properties.

   c. These models need to be developed for 3D analysis, eg. for the study of conditions around penetrations.

A computational model was developed in this project.

5. Verification of the models

   a. Verification of the chemical and physical part of the models requires measurements to verify the models with. There are already cases where similar measurements as those needed in this case have been

performed, for instance in Barsebäck. Those results can be used to verify the models.

b. Verification should also be made by means of results from on-going measurements in Ringhals.

c. Measurements of the reduction of the pre-stressing forces of various tendons (horizontal, vertical, up / down) may in some cases be used to verify the moisture/shrinkage analysis.

It was not possible to verify the results from the prediction on the actual RC wall, therefore the verification was performed by using results from a Swedish PWR.

6. Predictions in 1D & 3D

   a. The future temperature and humidity conditions of the concrete wall of the RC were predicted in 1D at different cross sections. Such predictions were also performed 3D geometry of the RC.

The results of the investigation described in this section shall provide all information needed to determine the state of stress and strain at any location in the structure, caused by the variations in moisture and temperature conditions of the structure.

1.2 Objectives of this report

The objective of this report is to estimate the temperature and moisture distribution in a concrete wall of a RC. The estimations are based models on what was already available when the project started from a previous project in Sweden. Some improvements, however, has been d to be done.

The results of the early estimations are of course not very reliable but more demonstrates the principle conditions that could occur. The sub-project G4 works on significant improvements of this kind of predictions.

Magnus Åhs and Lars-Olof Nilsson at Lund University have developed the heat and moisture transfer model this project. Stéphane Poyet at CEA in Saclay, France performed the laboratory work of the replica concrete and evaluated its moisture properties. The approach has been discussed with Valérie L'Hostis and Stéphane Poyet at CEA in Saclay, France.

A first draft was sent to the coordinator of sub-project G3.1 Burkhard Wienand at Areva for a judgement whether the results met the requirements by G3.

In the second draft some changes in the input data were made: the initial moisture conditions and the thickness of the containment wall were corrected. A comment on the 3D-calculations was given. In this report all the results are included.

2 Computational model

The analyses, which included coupled heat and moisture balance equations, were performed in Comsol Multiphysics.

2.1 Heat balance model

The temperature conditions inside the RC concrete wall were determined by solving the conventional energy-balance equation, with constant heat conductivity and heat capacity and sine functions as boundary conditions, as described in chapter 3.2.

2.2 Moisture transport model with water vapour content as driving potential

In predictions of the moisture distribution in both a BWR and PWR performed earlier, the moisture transport model was based on the water vapour content [1], v, [kg/m^3] as the transport potential, cf. equation (1.1)

$$J = -\delta_v \frac{\partial v}{\partial x} \qquad (2.1)$$

where δ_v is the moisture transport coefficient [m^2/s], shown in Figure 2.1.

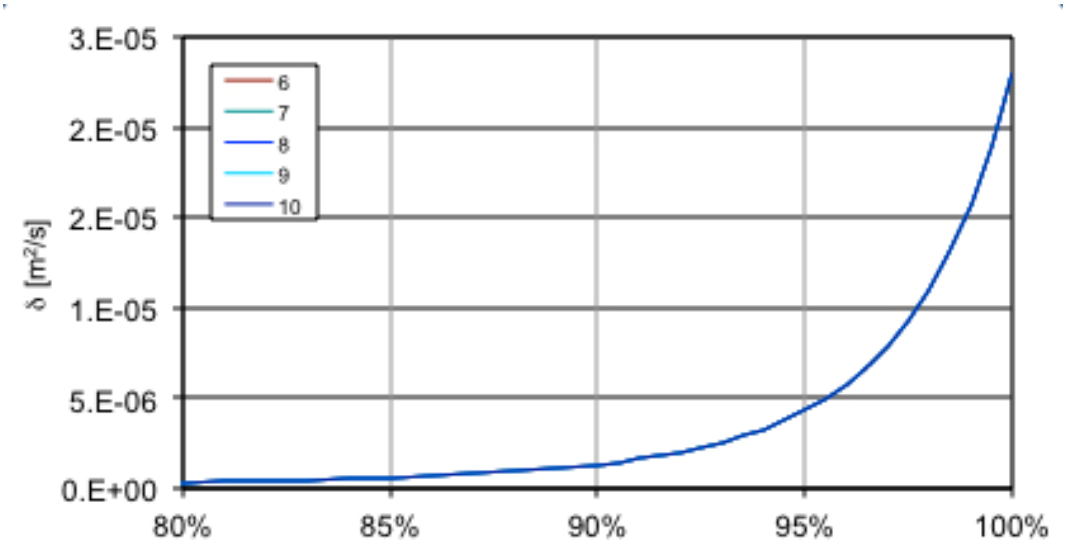

Figure 2.1 The moisture dependent moisture transport coefficient δ_v, [2]

Equation (1) was shown to give very good predictions, [1] for a BWR containment where moisture measurements could be done for comparisons. The BWR had very different temperature levels from top to bottom, but almost no temperature gradients through the walls.

Equation (1) was also used by [1] for a PWR containment wall with significant temperature gradients, cf. Figure 2.2.

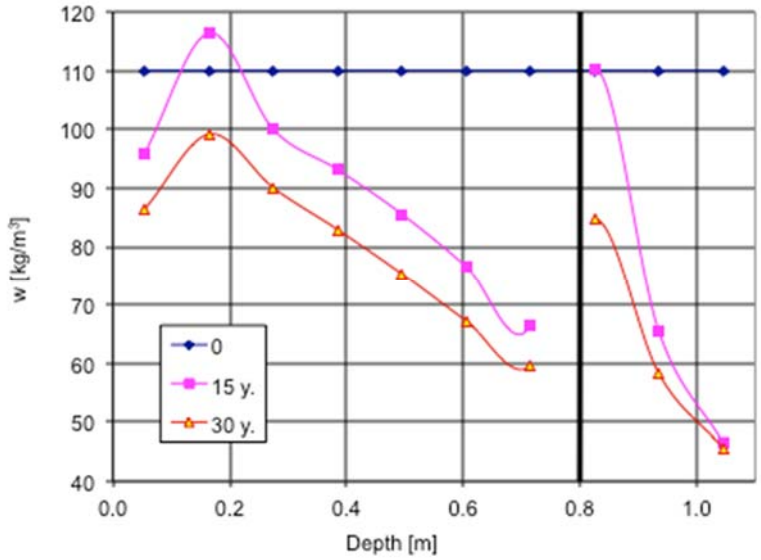

Figure 2.2 Predicted moisture profiles for a PWR containment wall, the thick black line represents a steel liner, [1]

Figure 2.2 shows the water content in the concrete material in kg moisture per cubic meter of concrete.

No measurements could be done for comparison at that time so the predictions were published with a large uncertainty. Recently, Oxfall [3] had an opportunity determine the moisture distribution of a concrete structure subjected to a significant temperature gradient during approximately 30 years, cf. Figure 2.3. Two moisture distributions was determined at this occasion. From these measurements it is quite obvious that equation (1) is not suitable for describing moisture transport under a temperature gradient. The water vapour content is not the correct transport potential.

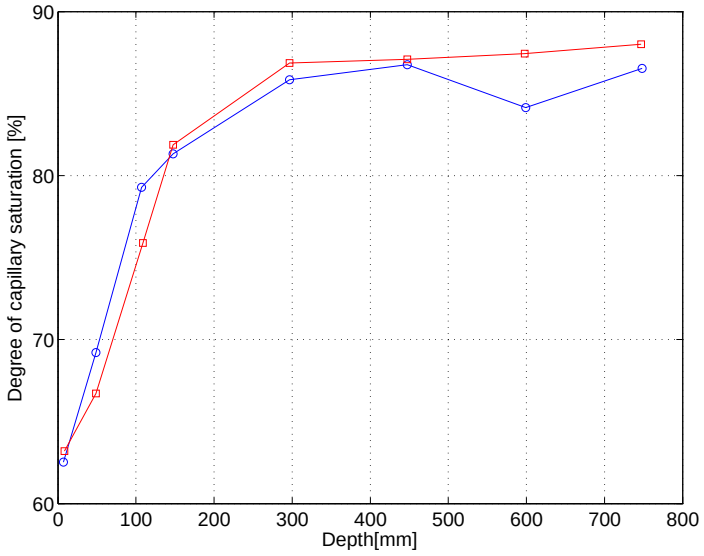

Figure 2.3 Measured moisture content profiles, as degree of capillary saturation, in a PWR containment wall after 30 years of drying under a temperature gradient, redrawn from [3]

2.3 Moisture transport model with air relative humidity as driving potential

A more accurate model should account for the temperature gradient and should use the relative humidity (RH), or the capillary pressure, as the transport potential. In the present analyses the RH has been chosen as the potential, see equation (2.2)

$$J = -\delta_\varphi \frac{\partial \varphi}{\partial x} \qquad (2.2)$$

where φ [kg/kg] is the RH in the pores of the material and δ_φ [m^{2}kg/(sm^3)] is the moisture dependent moisture transport coefficient with RH as the transport potential.

The moisture transport in the proposed model [4], is based on the mass conservation equation, Fick's second law, equation (2.3),

$$\frac{\partial W_e}{\partial t} = \frac{\partial \mathrm{W_e}}{\partial \varphi}\frac{\partial \varphi}{\partial \mathrm{t}} = \nabla\left(\delta_\varphi \nabla \varphi\right) + Q_2 \qquad (2.3)$$

where $\frac{\partial W_e}{\partial \varphi}$, represents the moisture capacity in [kg/m^3], φ represents the relative humidity in [-], δ_φ, represents the moisture transfer coefficient with RH as the driving potential in [m^{2}kg/(sm^3)], and Q_2, represents a source or a sink in [kg/m^3]. The sink may describe self-desiccation. However, self-desiccation is only roughly included in the suggested hygrothermal model. The self-desiccation is assumed to reduce the RH from 100% RH down to 92% RH throughout the structure. This drying has assumed to have taken place during the first 30 days after the RC was finished. The moisture capacity is derived from the desorption isotherm and is estimated as tangent of the desorption isotherm.

Now, the moisture transport coefficient δ_φ , see equation (2.4) can easily be calculated from δ_v,

$$\delta_\varphi = \delta_v \cdot v_s \qquad (2.4)$$

where v_s [kg/m^3]is the air water vapour content at saturation.

The temperature dependency of the moisture transport in equation (2.1) is due to the transport potential, the vapour content, being strongly temperature dependent. Now, the equally strong temperature dependent moisture transport in equation (2.2) is due to the temperature dependency of the transport coefficient, δ_φ. The transport coefficient δ_φ , is based on δ_v [2], see Figure 2.4.

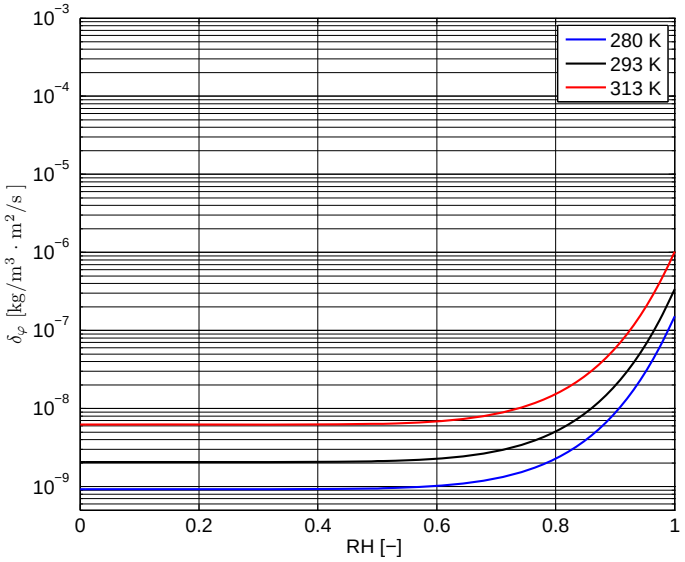

Figure 2.4 Temperature dependent moisture transport coefficient

2.4 Utilization of Comsol Multiphysics

The drying model has been applied in COMSOL Multiphysics. The model is a coupled heat and moisture transport. This means that the moisture properties are affected by the temperature and it is also possible to make heat transfer properties moisture dependent. The latter possibility was not used in this project, as the moisture dependency of the thermal properties is not of the same order of magnitude as is the temperature dependency of the moisture properties.

3 Input information

The input information regarding the boundary conditions are briefly described in this chapter. Most of it is from a report from a previous Swedish project, [1], where predictions were made for a similar case. A shorter version of the results from measurements of the boundary conditions is also available in English, [5].The material properties are based on the report but modified to also incorporate the temperature dependency.

The results of the 1D-predictions using the new model are shown in chapter 5 and the 3D-predictions are shown in chapter 7.

3.1 Geometry and material properties

Early predictions were made in 1D for the wall in a reactor containment wall, cf. Figure 3.1.

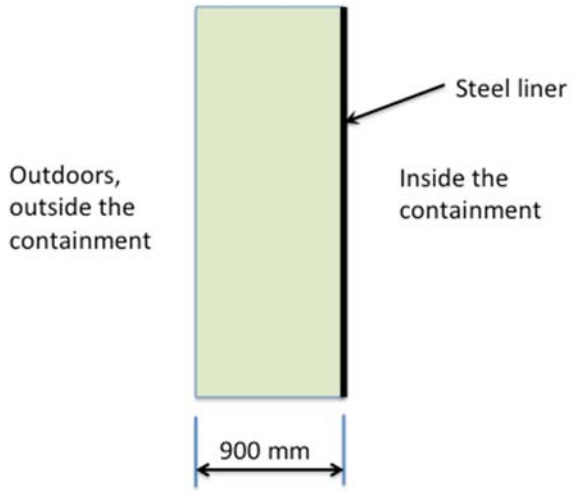

Figure 3.1 The containment wall with a steel liner

The dimensions were 900 mm concrete outside the steel liner and no concrete inside it.

The concrete was assumed to have a water-cement ratio of 0.5 and similar properties as the some 30-40 year old concretes in Swedish RC walls.

3.2 Boundary and initial conditions

The temperature condition inside the containment was assumed to be +40±8°C at the inner surface in the top of the containment, with an annual variation as a sine function, and +23±1°C at the bottom. The outdoor temperature was assumed to be +7±9°C at the outer surface, also with a sine function variation. The ground temperature was assumed to have a constant temperature of 11°C. RH at the outside surface was set to

80±8 % RH. The RH inside the containment wall will have no influence on the moisture conditions outside the steel liner. The RH at the RC inside surface was set to 30±3.5 %. The relative humidity under the foundation was assumed to have a constant relative humidity of 95% RH. Heat and moisture resistances at the surfaces were neglected.

The boundary conditions are shown in Figure 3.2. The dimension on the x axis is days in both figures and the dimension on the y-axis in the upper diagram is temperature in °C and in the lower diagram relative humidity.

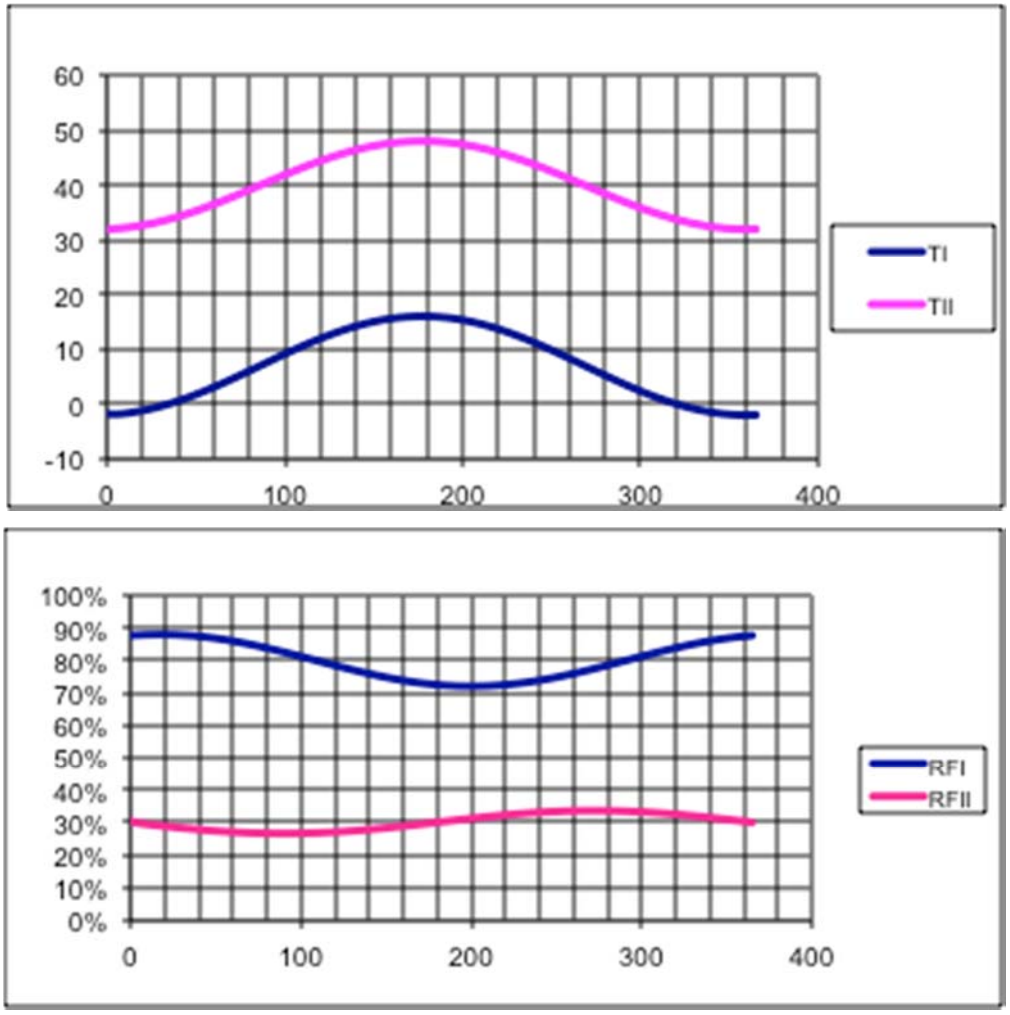

Figure 3.2 Boundary conditions at the two surfaces: temperatures (top) at the inner (TII) and outer (TI) surface and RH (bottom) at the outer (RFI) and inner (RFII) surface.

The initial temperature conditions were set to +20°C; they will only matter for the first couple of days. The initial moisture conditions were set to an

RH of 92 %, corresponding to the moisture content after self-desiccation for a couple of years of construction.

3.3 Material properties

The decisive material properties for the moisture transport analysis are desorption isotherms, moisture transport coefficients, the heat capacity and the heat conductivity. These properties were estimated by using different methods since it was not possible to acquire them from an actual RC wall.

3.3.1 Desorption isotherms

A number of desorption isotherms were used in this study.

One of the desorption isotherms was modelled from Nilsson [6] for a concrete with a w/c of 0.5 and a cement content of 307,2 kg/m^3. This desorption isotherm was used both in the 1D predictions and the sensitivity analysis of the 3D predictions. From the previous predictions it was obvious that the temperature dependency of the desorption isotherm is a decisive parameter.

Temperature dependent desorption isotherms were constructed by adding/subtracting a certain, temperature dependent moisture content to/from the desorption isotherm at +20 °C. This was done with a sine function with a value zero at RH = 0 and 100 % and with an amplitude of (293.15-T)/2 kg/m3 at 50 % RH see equation (3.1).

$$W_{eT} = \frac{293.15-T}{2} \cdot \sin(RH \cdot \pi) \qquad (3.1)$$

The dashed lines in Figure 3.3 show how the ability to contain moisture changes with respect to a temperature change. See for example how a change of 13K affects the ability to contain water. A change from 20 °C to 7 °C increases the materials ability to contain moisture at 50 % RH to 6.57 kg/m3 (293.15-280)/2, see the blue dash dotted line. The amplitude was estimated from data by Poyet and Poyet and Charles [7, 8].

The desorption isotherms at some temperature levels are shown in Figure 3.3.

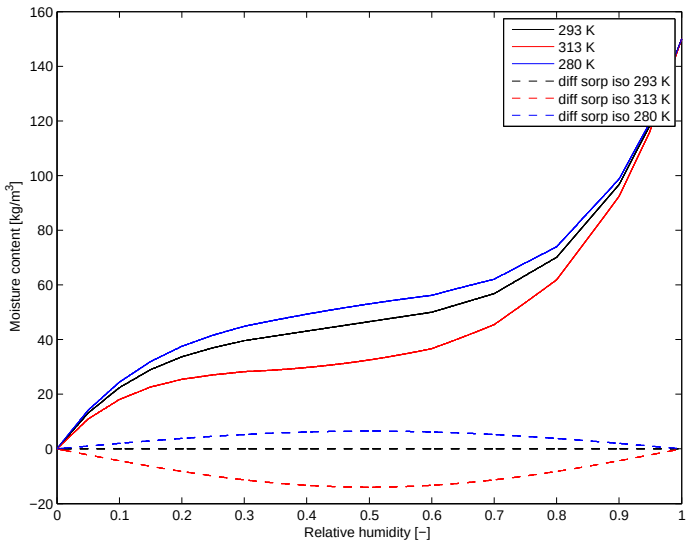

Figure 3.3 The desorption isotherms at three different temperatures.

Another desorption isotherm, see Figure 3.4, was used at a later stage in this project in the simulation with and without rain. This desorption isotherm was a preliminary estimation; see section 4.4.1, which was an early estimation quantified from the measurements performed on the replica concrete. This estimation was used in the simulation with and without rain.

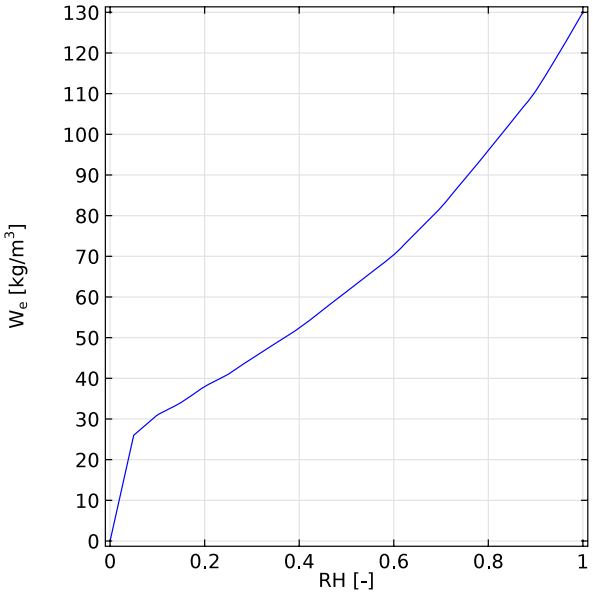

Figure 3.4 Preliminary estimation of the desorption isotherm assessed from the replica concrete.

When the experiments on the replica concrete were finished; a final set of moisture properties was assessed. The desorption isotherm is shown in Figure 3.5.

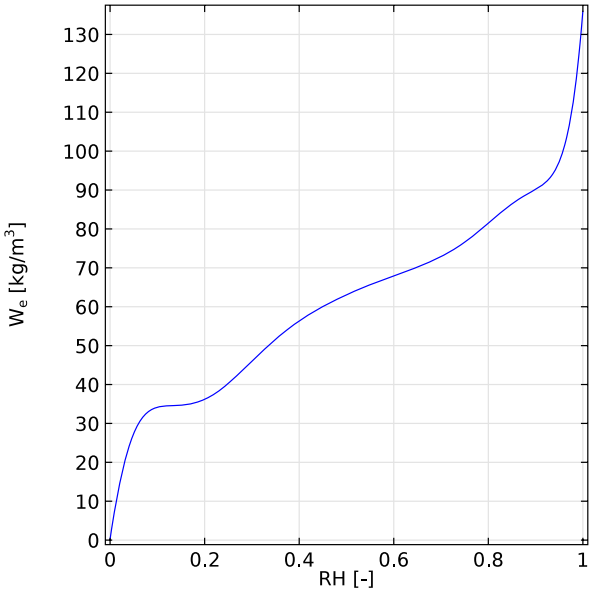

Figure 3.5 Desorption isotherm assessed from the replica concrete.

3.3.2 Diffusion coefficients

Three different diffusion coefficients were used in the analyses.

The diffusion coefficient, δ_φ, used in the 1D simulations and the sensitivity analysis in 3D, was adopted from the literature [2], see Figure 3.6. Please note that this diffusion coefficient is shown at three different temperatures.

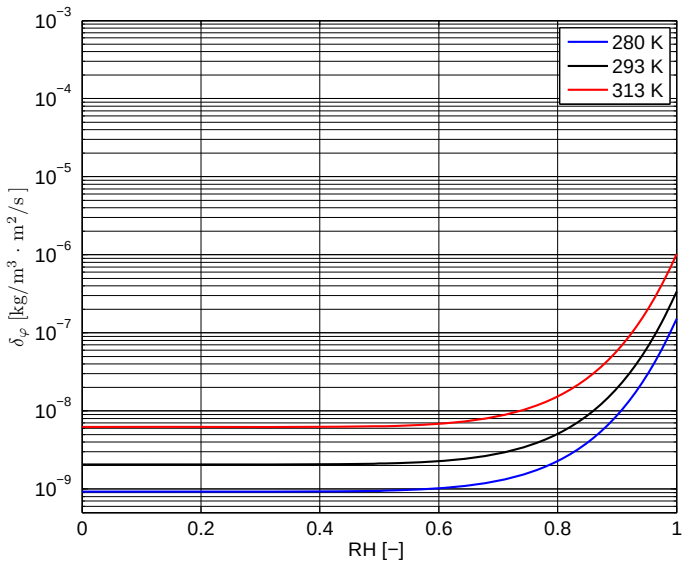

Figure 3.6 Temperature dependent moisture transport coefficient adopted from [2].

Another diffusion coefficient was determined before the experimental test of the replica concrete was finalized. This preliminary estimation of the diffusion coefficient is displayed in Figure 3.7.

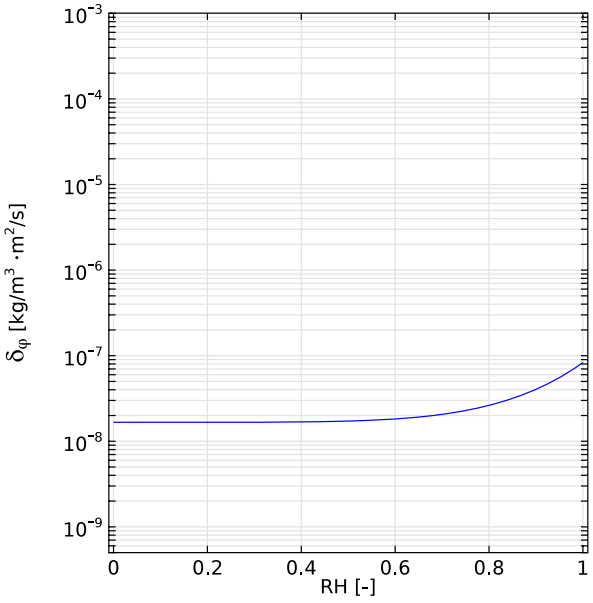

Figure 3.7 Preliminary estimation of the diffusion coefficient assessed from the replica concrete

The diffusion coefficient that was determined after the completion of the laboratory experiment is shown in Figure 3.8.

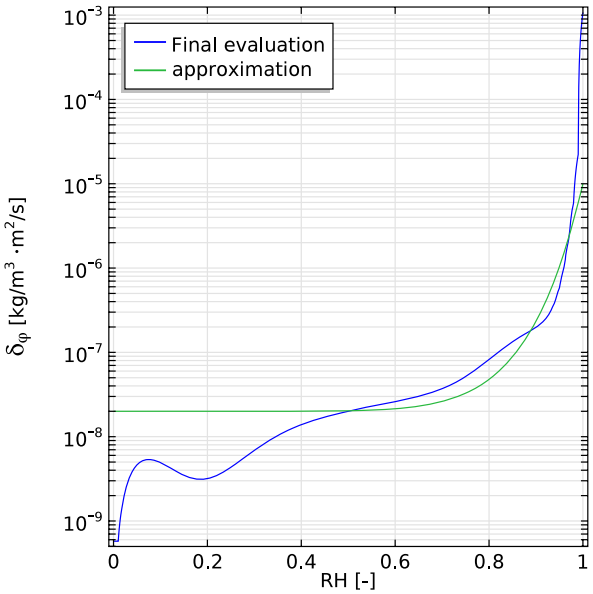

Figure 3.8 The diffusion coefficient assessed from the replica concrete

For clarity the presented diffusion coefficients are shown in Figure 3.9, at a temperature of 20 °C.

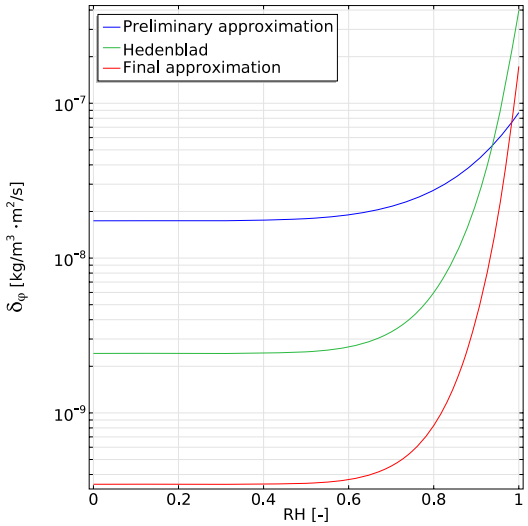

Figure 3.9 Diffusion coefficients used in the simulations

3.3.3 Thermal properties

The heat conductivity for the concrete was set to 1.4 W/mK and the heat capacity to 880 J/kgK. This means that the moisture dependency of the heat conductivity was neglected.

4 Unsaturated moisture transport properties of the replica concrete

This chapter briefly reports the work done to assess the moisture properties of the RC concrete by using a replica concrete instead of using extracted concrete samples from a real RC.

4.1 Material

The reactor containment was built in the late 70s (between august 1977 and January 1979). The water to cement ratio of the original concrete was 0.45. A compressive strength larger than 40 MPa was specified for the original concrete (prestressed concrete). The mix proportion of the original concrete is shown in **Table 4.1**.

Table 4.1: Mix proportions of the original concrete.

Compound	Nature/origin	Quantity
Cement	CPA 400, Cantin (Ciments Français)	400 kg/m^3
Water		180 kg/m^3
Sand 0/3	Rounded dune sand	140 kg/m^3
Sand 0/4	Crushed limestone	480 kg/m^3
Gravel 3/8	Crushed limestone	370 kg/m^3
Gravel 10/25	Rounded	815 kg/m^3
Super plasticizer	Plastiment BV40 (Sika)	0.4% of C

It was not allowed to drill cores from the considered RC and there were no spare specimens left of the original concrete. It was then decided to make a replica of the concrete in the laboratory. Unfortunately, none of the original raw materials were available. Each of them was therefore replaced with similar, modern and easily accessible surrogate material. The mix proportion of the replica concrete is shown in **Table 4.2**. The super plasticizer content (Master Glenium 27) was adjusted so that the fresh mix was easily poured (slump = 175 mm).

Table 4.2: Mix proportions of the replica concrete.

Compound	Nature/origin	Quantity
Cement	CEM I 42.5 Dannes (Holcim)	400 kg/m^3
Water		180 kg/m^3
Sand 0/4	Crushed limestone sand	620 kg/m^3
Gravel 4/8	Rounded limestone	370 kg/m^3
Gravel 7/25	Rounded marble	815 kg/m^3
Super plasticizer	Master Glenium 27 (BASF)	0.1% of C

Twenty cylindrical specimens (Ø11×22 cm) were produced in one batch (50 litres). They were unmoulded two days after casting and cured in lime water. The compressive strength was measured at 28 and 90 days following current recommendations (standard EN 12390-1). Six specimens were tested each time. The results were compared to those obtained during the construction, Figure 4.1. The new concrete was found to have a higher strength than that of the considered RC. The use of the modern cement may have an increased hydration rate and strength. The difference between field- and laboratory manufactured concrete may also explain this difference.

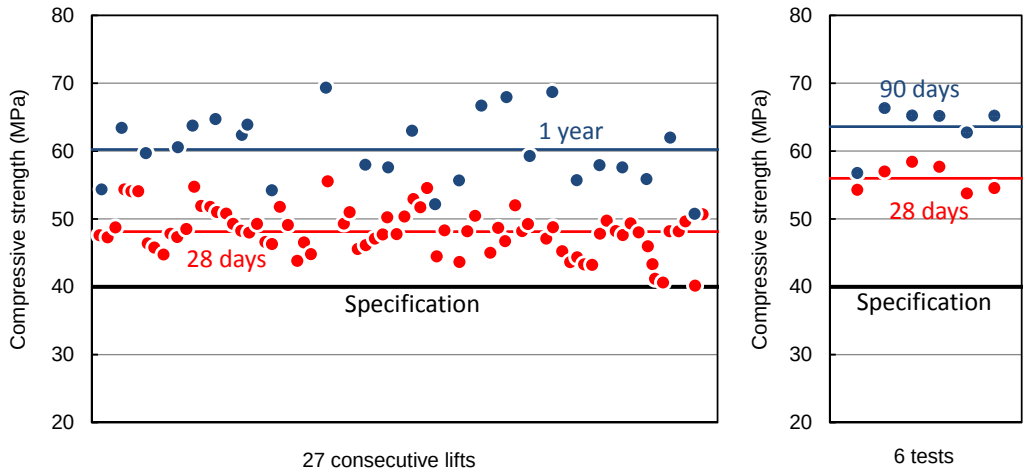

Real structure Laboratory

Figure 4.1 Compressive strength

4.2 Methods

Three cylindrical specimens (Ø113×226 mm) were taken out of cure and sawn in six parts 210 days after casting. Each of these three cylinders was then cut into five thin discs (about 10 mm) and one thick disc (55 mm). The fifteen thin discs were then used for the determination of the desorption isotherm whereas the three thick discs were used for the assessment of the water transport property.

All these samples were first vacuum saturated. The specific gravity of the concrete d_{sat} was measured using the buoyancy method and the porosity $\emptyset$ was obtained using oven-drying at 105°C. The pore size distribution was investigated by mercury intrusion porosimetry (MIP) using a Micrometrics Autopore IV. Samples were crushed into small pieces (several millimetres), frozen by immersion into liquid nitrogen, let to dry under vacuum for seven days and then tested at 20 ± 2°C.

The desorption isotherm was characterized using a sorption balance (SMS DVS Advantage). Thin disks were crushed and then powdered in a CO_2-free glove box and then sieved to remove the particles larger than 100 µm. The powder was saturated using deionized water and a sample of about 50 mg was taken and introduced into the sorption balance. The tests were performed at 25°C ± 0.1°C. The RH was gradually decreased in steps under the "dm/dt" mode (the balance software automatically shifted from one RH step to another when equilibrium was considered to be reached).

The water transport property was evaluated using inverse analysis: the intrinsic permeability (K) was fitted through numerical simulations to match experimental data [9, 10]. Here, the three initially saturated disks (Ø113×55 mm) were subjected to drying at 55% RH and 25°C in a climatic chamber during 100 days. The finite-element code Cast3m[1] was used to solve equation (4.1):

$$\emptyset\left(\frac{\partial S}{\partial P}\right)\frac{\partial P}{\partial t} = div\left[K\frac{k_r}{\eta}\underline{grad}(P)\right] \qquad (4.1)$$

where

- P is liquid water pressure [Pa];
- S saturation index [-];
- η water viscosity [Pa s];
- k_r relative permeability to water [-].

The pressure P was calculated using Kelvin-Laplace equation:

$$P(h) = -\rho\frac{RT}{M}ln(h) \qquad (4.2)$$

[1] http://www-cast3m.org

where

- ρ is water density [kg/m^3];
- R gas constant [J/mol/K];
- T absolute temperature [K];
- M water molar mass [kg/mol];
- h relative humidity.

For more detail about the assessment procedure, the reader is referred to Poyet et al. [11, 12].

4.3 Experimental results

The concrete porosity was found to be equal to 12.6% and the specific gravity, the ratio of the (saturated) concrete density to the water density, was found to be 2.48, see Table 4.3. The variability was small, the coefficient of variation (COV) is the ratio of the standard deviation to the mean. It is a measure of dispersion of datasets.

Table 4.3 Porosity and specific gravity.

	Mean value	Min/Max	Standard dev	COV
Porosity Ø	12.6%	12.0%/13.5%	0.9%	7%
Specific gravity d_{sat}	2.48	2.46/2.49	0.02	1%

The desorption isotherm is shown in Figure 4.2. Two tests were conducted using two samples taken from two different disks. Here again, the variability remained limited (the two curves overlap). The fall in saturation at high RH (between 100% and 95%) could be due to the presence of big pores (between 0.1 and 10 µm) as observed using Mercury Intrusion Porosimetry (MIP), Figure 4.3.

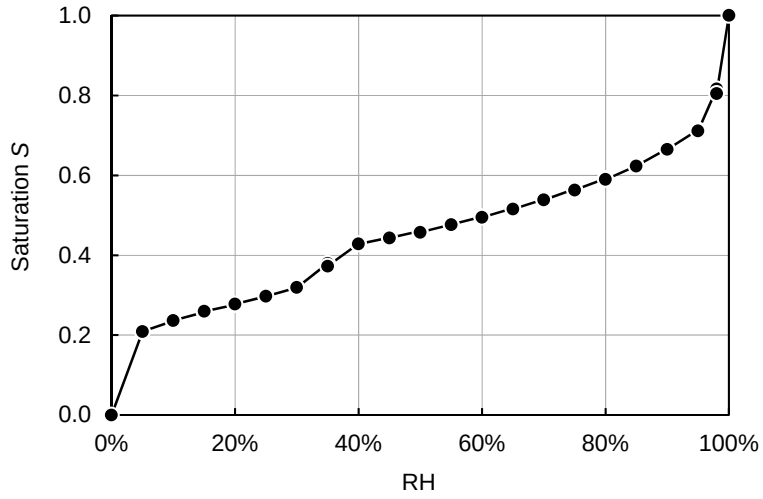

Figure 4.2 Desorption isotherm

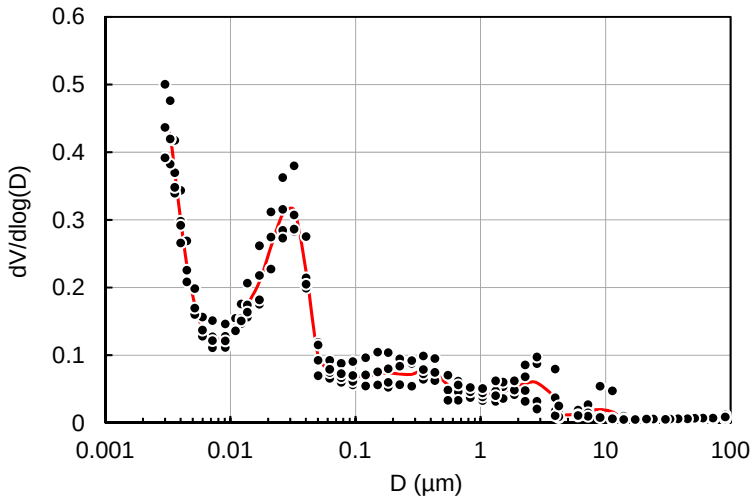

Figure 4.3 Pore size distribution using MIP (4 different samples were tested).

The mass loss evolution of the big disks (Ø113×55 mm) subjected to drying at 25°C and 55% RH is shown in **Figure 4.4**.

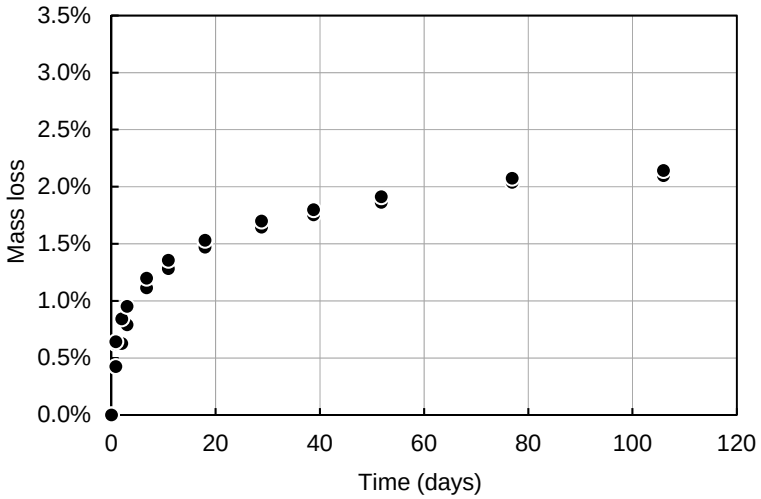

Figure 4.4 Drying at 25°C and 55% RH.

4.4 Permeability evaluation

4.4.1 Mualem-van Genuchten

The inverse analysis was first conducted in a classical way using Mualem-van Genuchten model [13, 14]. Van Genuchten equation (4.3) was used to fit the desorption isotherm **Figure 4.5**.

$$S(P) = \left[1 + \left(\frac{P}{P_0}\right)^{\frac{1}{1-m}}\right]^{-m} \quad \text{with} \quad P(h) = -\rho\frac{RT}{M}ln(h) \tag{4.3}$$

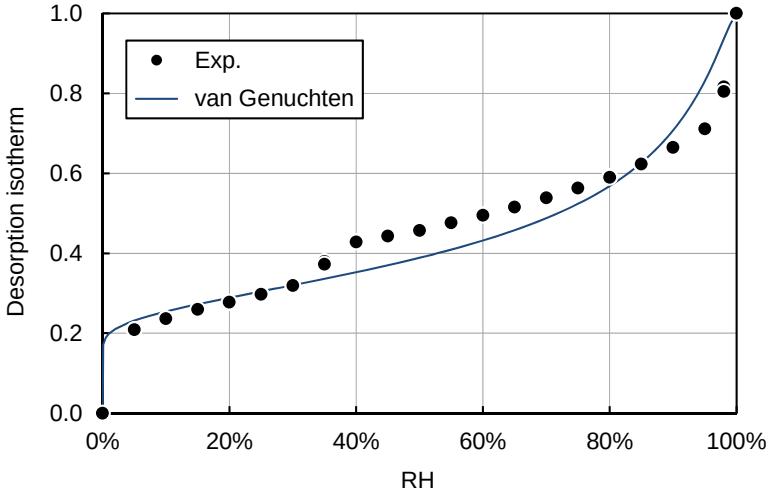

Figure 4.5 desorption isotherm described using van Genuchten equation.

One can notice that the fit is not very good: the 'predicted' isotherm deviates from the experimental results at high RH and between 40% and 80%. The latter is important because the drying experiment was conducted at 55% RH. The two van Genuchten parameters P_0 and m are shown in **Table 4.4**.

Table 4.4 van Genuchten parameters.

	P_0	m
Value	6.94 MPa	0.263

The relative permeability k_r was estimated using Mualem's model [14]:

$$k_r(P) = \left[1 + \left(\frac{P}{P_0}\right)^{\frac{1}{1-m}}\right]^{-\frac{m}{2}} \left\{1 - \left(\frac{P}{P_0}\right)^{\frac{1}{1-m}} \left[1 + \left(\frac{P}{P_0}\right)^{\frac{1}{1-m}}\right]^{-m}\right\}^2 \qquad (4.4)$$

Figure 4.6 illustrates the numerical restitution of the mass loss evolution for five different intrinsic permeability (K) values (from 2×10^{-21} to 35×10^{-21} m^2). The intrinsic permeability was evaluated by minimization of the quadratic difference between the computed and measured mass loss see **Figure 4.6**, 15×10^{-21} m^2.

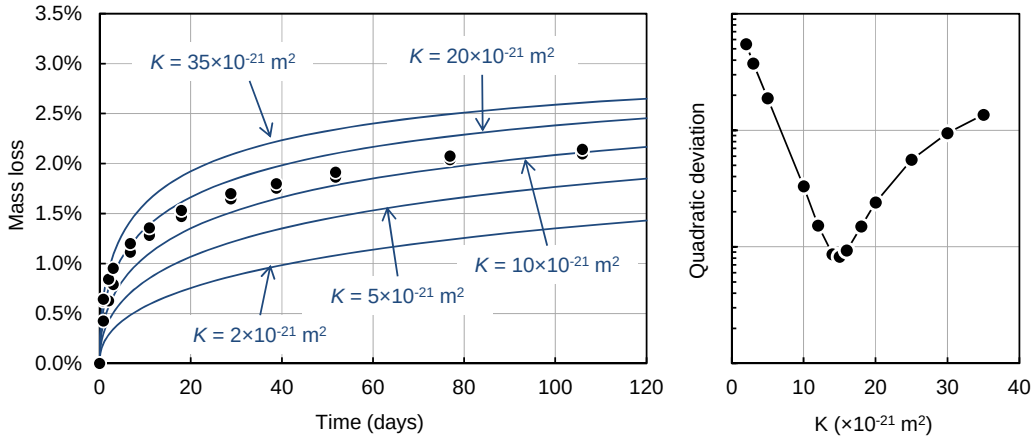

Numerical restitution of the mass loss evolution

Least-square minimization process

Figure 4.6 Permeability evaluation using van Genuchten equation.

4.4.2 Polynomial

An alternative to the van Genuchten method is the use a polynomial fit to describe the desorption isotherm. This method was used by using a 10^{th} order polynomial to fit the experimental data of the desorption isotherm:

$$S(h) = \sum_{n=0}^{10} a_n h^n \qquad (4.5)$$

The quality of the description was greatly improved **Figure 4.7**. The corresponding polynomial parameters are shown in **Table 4.5**.

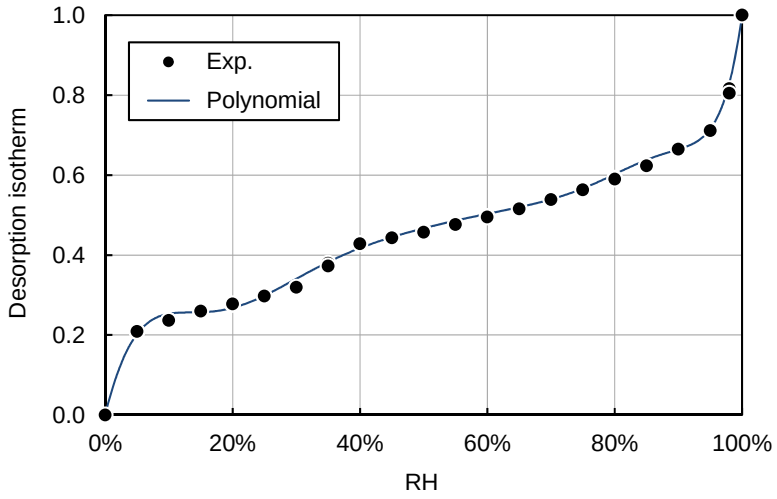

Figure 4.7 Desorption isotherm described using a 10th order polynomial.

Table 4.5: Polynomial parameters.

	Value
a_0	7.93×10^{-5}
a_1	3.47×10^{-1}
a_2	-3.01×10^{0}
a_3	7.79×10^{0}

	Value
a_4	3.38×10^{1}
a_5	-2.84×10^{2}
a_6	8.53×10^{2}
a_7	-1.40×10^{3}

	Value
a_8	1.33×10^{3}
a_9	-6.88×10^{2}
a_{10}	1.49×10^{2}

In this specific case the relative permeability was once more estimated using Mualem's model and the trapezoidal form of Riemann sums; see Poyet [11] for more detail. The intrinsic permeability was then evaluated to 18×10^{-20} m^2.

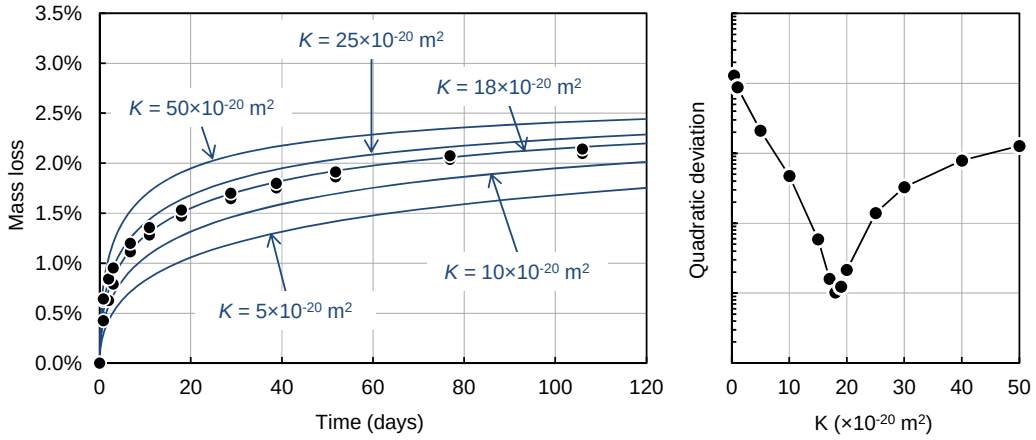

Numerical restitution of the mass loss evolution

Least-square minimization process

Figure 4.8 Permeability evaluation using polynomial.

4.4.3 Discussion

Using different equations for the description of the desorption isotherms yielded a significant difference of the intrinsic permeability value (by one order of magnitude). In inverse analysis, the intrinsic permeability depends on the input data [11]. This is due to the use of two different relative permeability evaluations (resulting from the use of two different desorption isotherms, **Figure 4.9**-a). Despite this difference, the two effective permeability evaluations tend to describe a unique curve that is believed to be representative of the unsaturated permeability of the concrete, see **Figure 4.9**-b.

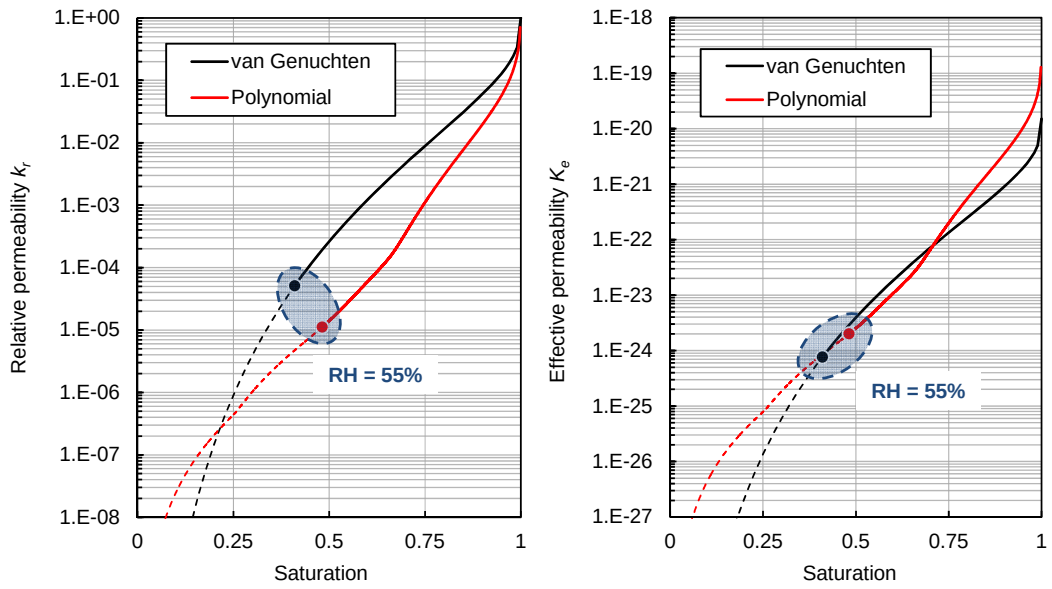

a - Relative permeability b - Effective permeability

Figure 4.9: Comparison of the relative and effective permeability.

The determination of the moisture properties of the replica concrete was not finalized until late in March 2015. Therefore it was not possible to use the final version of the determined moisture properties in any simulation. There was an attempt to perform an early prediction of the moisture properties of the replica concrete and these were used in one simulation which is presented, in section 7.2. The polynomial fitted desorption curve was used in one simulation, because it was not finalized until March 2015.

5 Predicted temperature and moisture distributions based on 1D-simulations

One-dimensional simulations were made for the top and the bottom parts of the containment wall with preliminary modelled moisture properties, see section3.3. The results are shown here. These two parts of the containment wall represent two different cases. One case was chosen near the base of the reactor containment wall, with a moderate temperature difference between outdoor and indoor conditions. The other case was chosen at a level of about 20 meters, with a larger temperature difference between the outdoor and indoor climate. All simulation results are based on calculations using the relative humidity, RH, as a driving potential.

5.1 Top of the containment wall, first 30 years

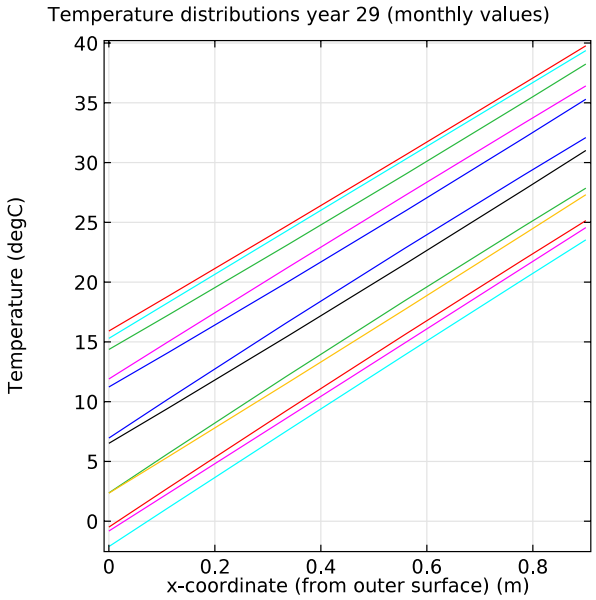

Figure 5.1 Temperature distributions at the top of the containment wall during the 29th year. Each curve represents one month during the year.

Obviously, the annual temperature variations on the two sides are so slow that the temperature profiles are almost linear all the time.

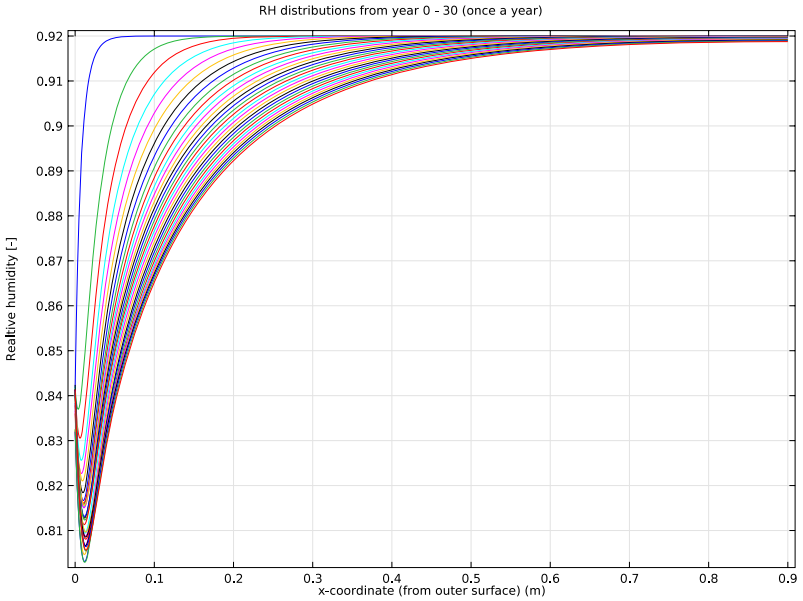

Figure 5.2 RH-distributions at the top of the containment wall during the first 30 years. Each curve represents one year, starting 92 % RH and drying towards the left surface

The RH-variations in the outer centimetres are due to the annual RH-variation in the outdoor air.

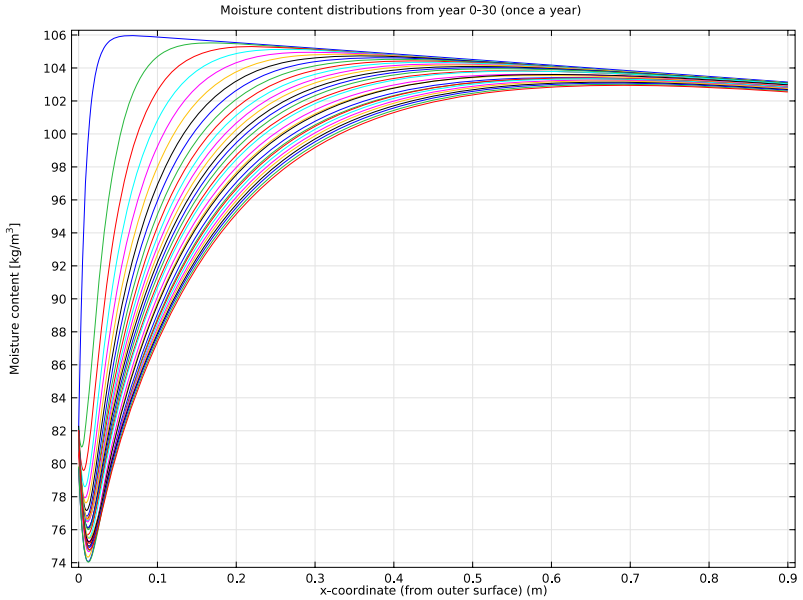

Figure 5.3 Moisture content distributions at the top of the containment wall during the first 30 years. Each curve represents one year.

The initial moisture content profile starts at around 106 kg/m^3 at the outer surface and around 103 kg/m^3 at the inner surface. This is not quite

correct but follows from the assumption of the initial RH being 92 % and the temperature dependency of the desorption isotherm. The initial moisture content profile is not uniform because the setpoint RH is 92% RH and the initial temperature profile is not uniform. This is corrected in the performed 3D calculations. This is done by setting an initial uniform temperature as well as a uniform humidity profile.

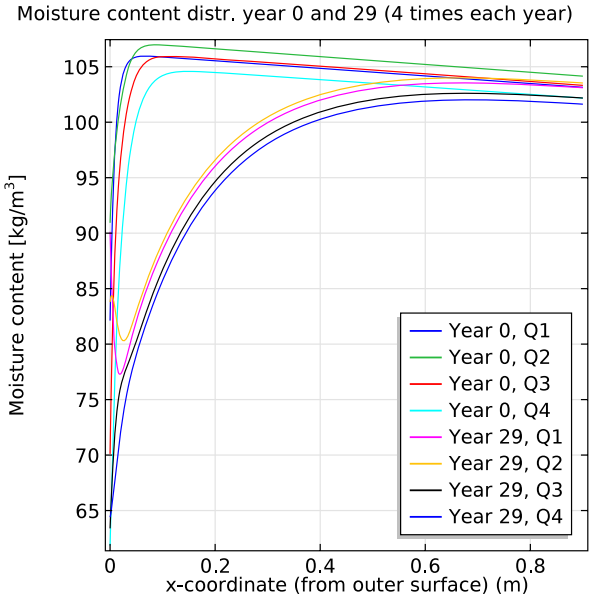

Figure 5.4 Moisture content distributions at the top of the containment wall during year 0 and the 29th year. Each curve represents every third month during these two years.

The moisture content at the steel plate, at x-coordinate 0.9 m, is not constant through a one year cycle, see Figure 5.4. This change in moisture content is not originating from moisture transport. The moisture content is derived from the desorption isotherm which is temperature dependent. At a RH of for example 90% RH the moisture content is higher at a lower temperature than at a higher temperature, this is why the moisture content is changing at the steel plate. Please note that the moisture content is not the driving potential, it is the RH.

5.2 Top of the containment wall, next 30 years

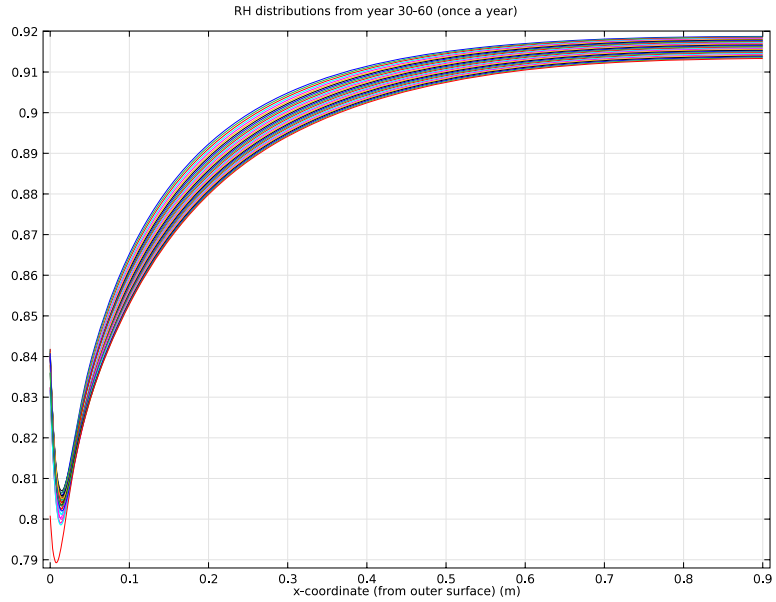

Figure 5.5 RH-distributions in the top of the containment wall during the years 30-60. Each curve represents one year, starting from the distribution after 30 years

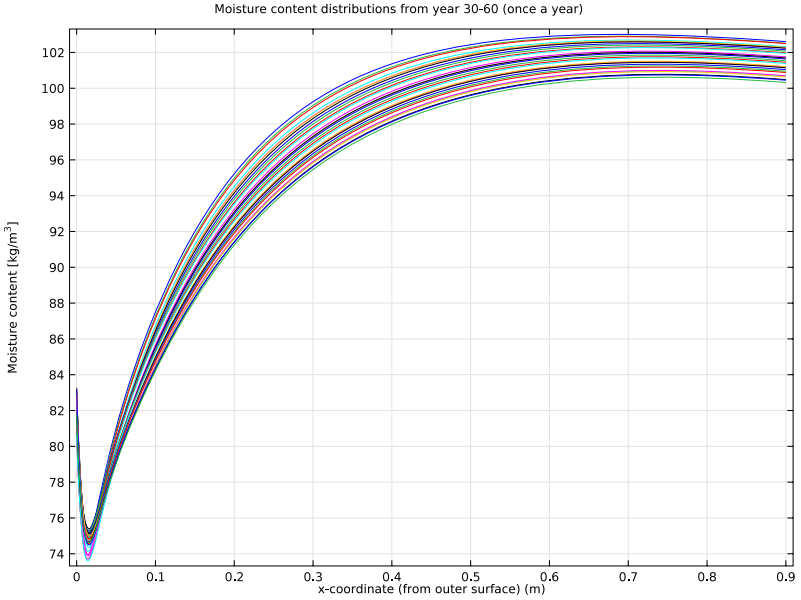

Figure 5.6 Moisture content distributions in the top of the containment wall during the years 30-60. Each curve represents one year, starting from the distribution after 30 years

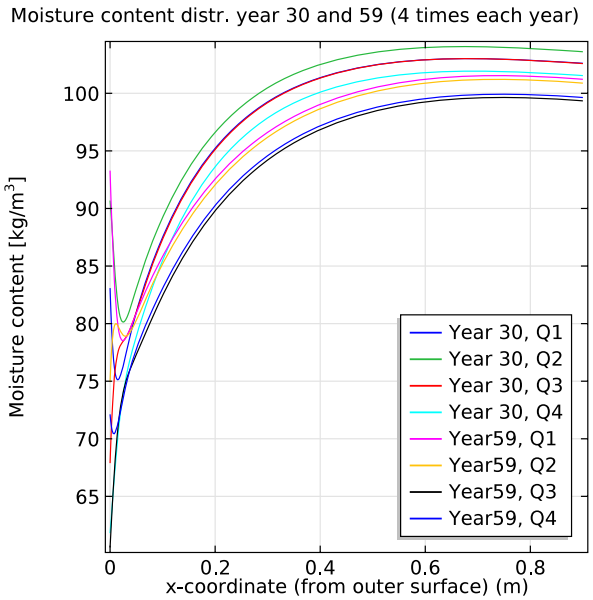

Figure 5.7 Moisture content distributions in the top of the containment wall during the 30th and the 59th year. Each curve represents every third month,Q1-Q4, during these two years.

5.3 Bottom of the containment wall, first 30 years

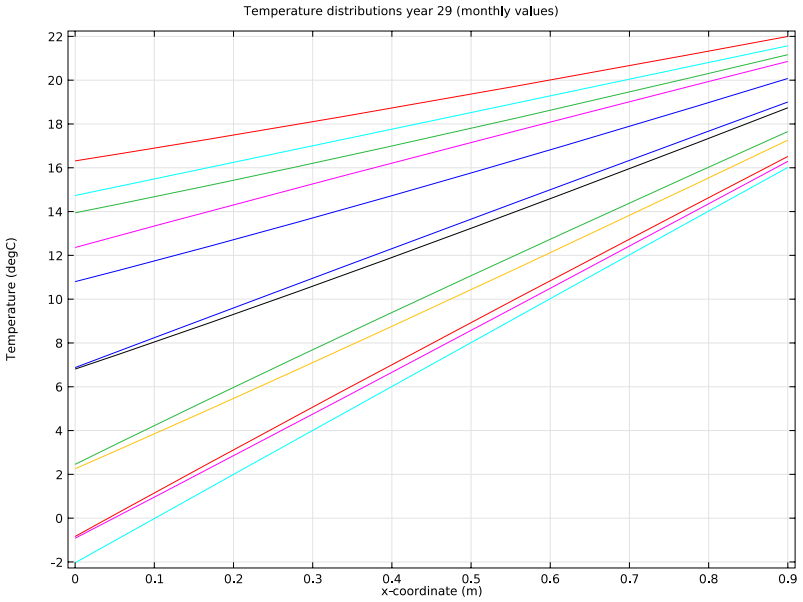

Figure 5.8 Temperature distributions in the bottom of the containment wall during the 29th year. Each curve represents one month during the year.

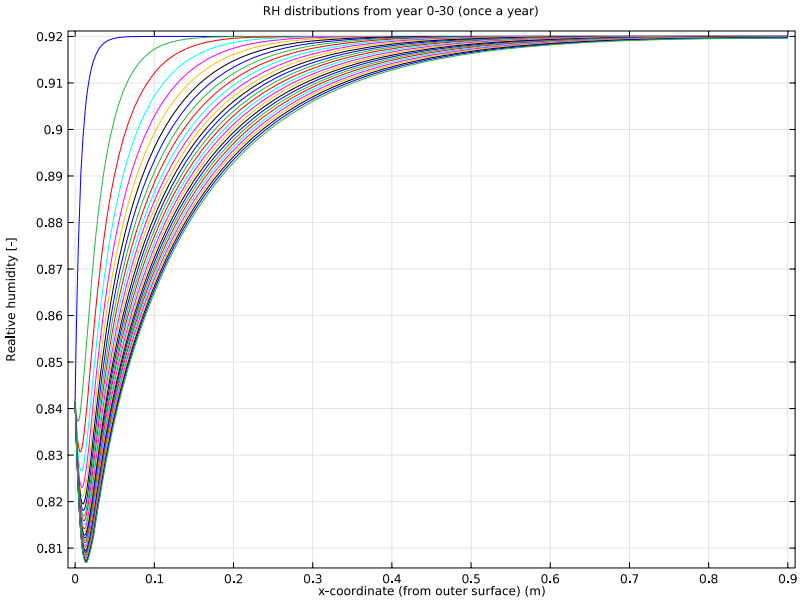

Figure 5.9 RH-distributions in the bottom of the containment wall during the first 30 years. Each curve represents one year, starting 92 % RH and drying towards the left surface

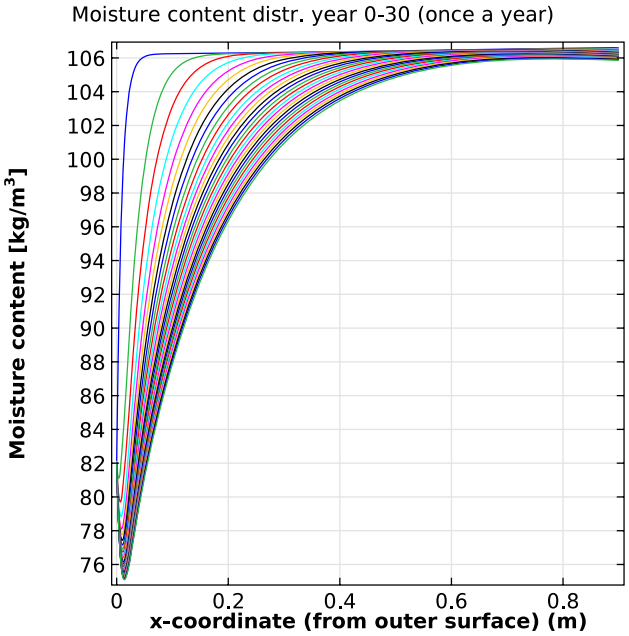

Figure 5.10 Moisture content distributions in the bottom of the containment wall during the first 30 years. Each curve represents one year, starting 92 % RH and drying towards the left surface

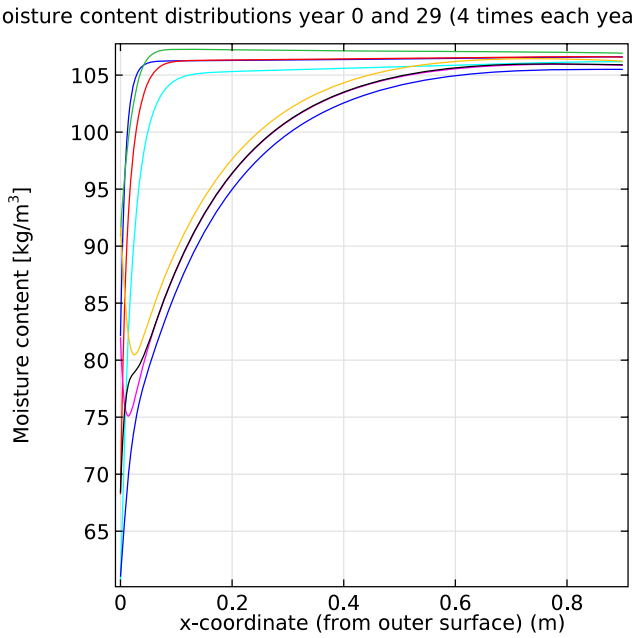

Figure 5.11 Moisture content distributions in the bottom of the containment wall during year 0 and the 29th year. Each curve represents every third month, Q1-Q4, during these two years.

5.4 Bottom of the containment wall, next 30 years

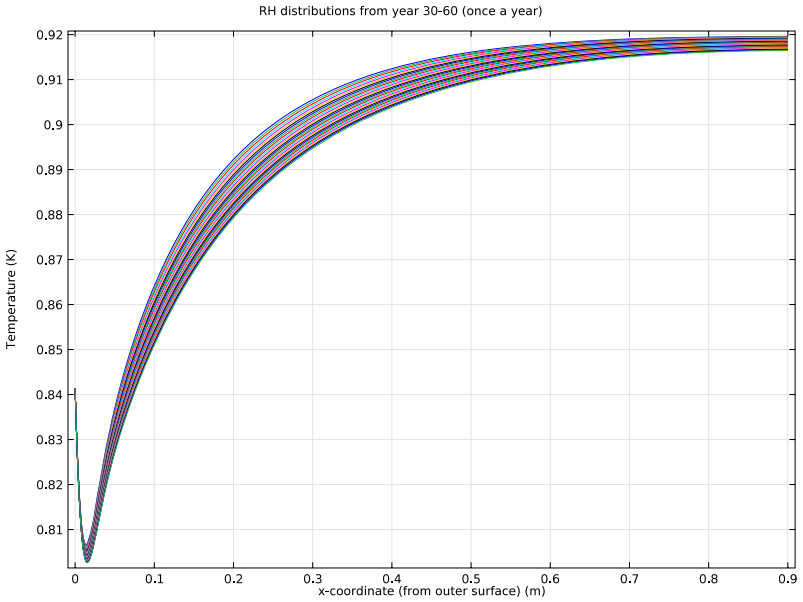

Figure 5.12 RH-distributions in the bottom of the containment wall during the years 30-60. Each curve represents one year, starting from the distribution after 30 years

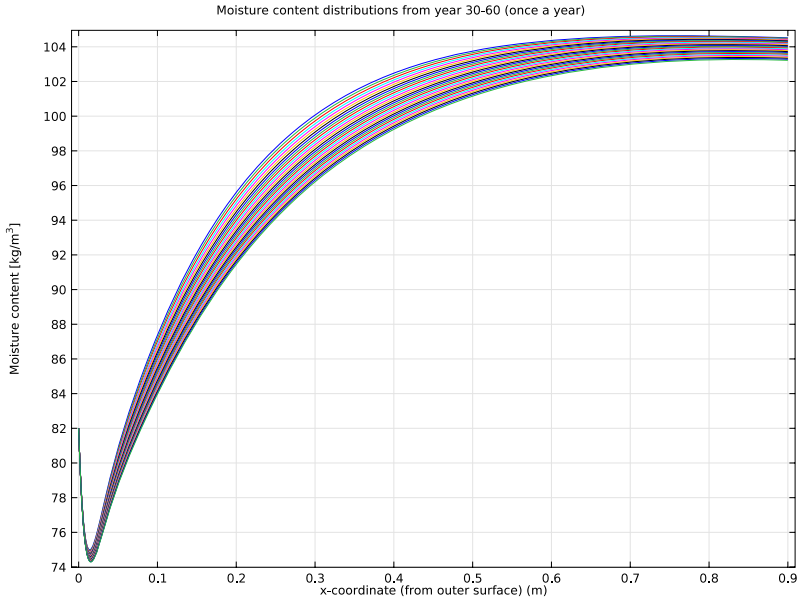

Figure 5.13 Moisture content distributions in the bottom of the containment wall during the years 30-60. Each curve represents one year, starting from the distribution after 30 years

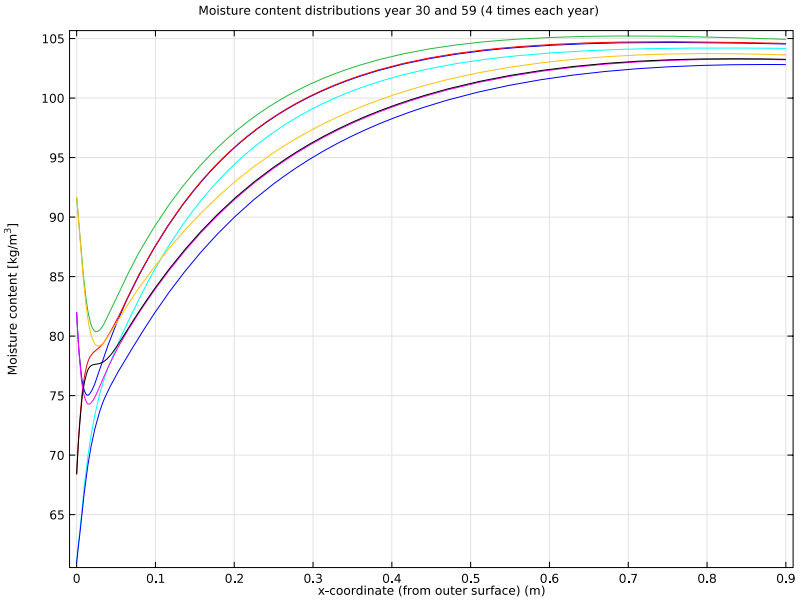

Figure 5.14 Moisture content distributions in the bottom of the containment wall during the 30th and the 59th year. Each curve represents every third month during these two years.

6 Moisture and temperature distribution in a 3D geometry

A model of the containment geometry is made in project G3 by using the Abacus software. Such a geometry has been made available for project G4 and it is possible to “import” it into the calculation software, Comsol Multiphysics.

A number of attempts have been made to use the 3D-model in our moisture calculation model. Finally, it was successful. The 3D-drawing from G3 can be used as the geometry for the moisture and temperature calculations. The geometry shown in Figure 6.1, is a first draft of the containment and a surrounding air volume, the air volume were not used for the simulation. This draft was not used for the simulations but represents a preliminary result of the geometry transfer from KTH in project G3 to Lund university.

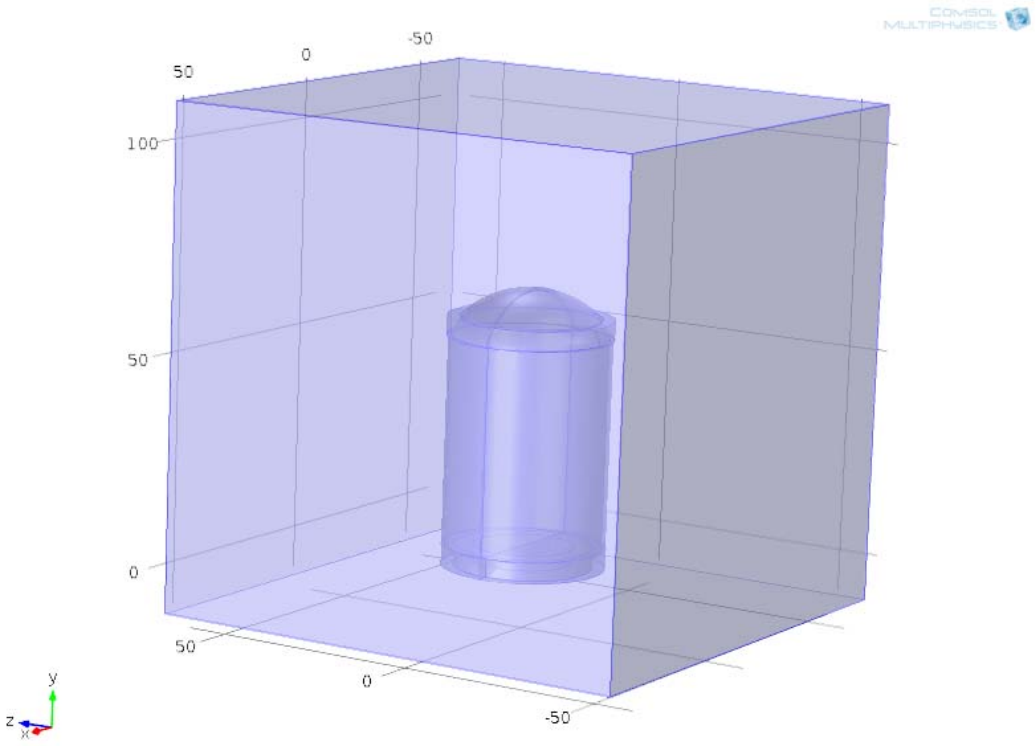

Figure 6.1 A 3D-geometry of the reactor containment surrounded by a volume of air.

In Figure 6.2 there is a graphical representation of the finalized 3 D geometry that was delivered from the G3 project.

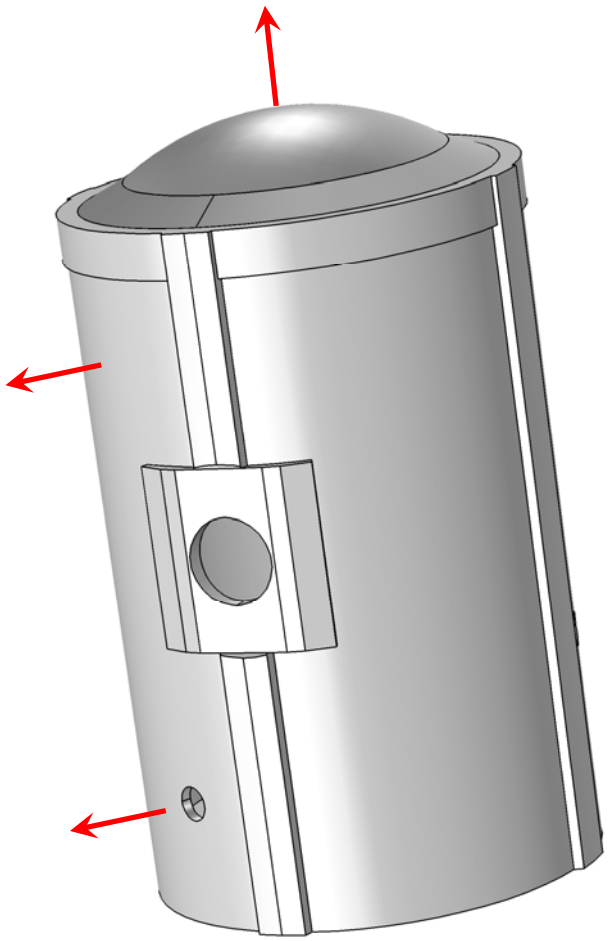

Figure 6.2 Finalized geometry of the reactor containment, shown as a solid, with two holes marking the access to the reactor containment. The red arrows indicate the position of the cross sections.

The RC has three large openings in the vertical wall, see Figure 6.2. They are situated at different locations of which two are shown; the last one, of a similar size as the other two, is at the opposite side of the RC. In addition there are four vertical ribs with a thicker cross section. Furthermore there is a maintenance tunnel around the foundation that is included in the geometric model, this is not visible in the figure. The red arrows indicate the location of the three different cross sections of the calculated moisture distribution (dome top, 10 m and 40 m above the foundation).

The mesh was configured as a fine free tetrahedral mesh with additional boundary layers at the outside surfaces. This quality of the mesh is shown in Figure 6.3.

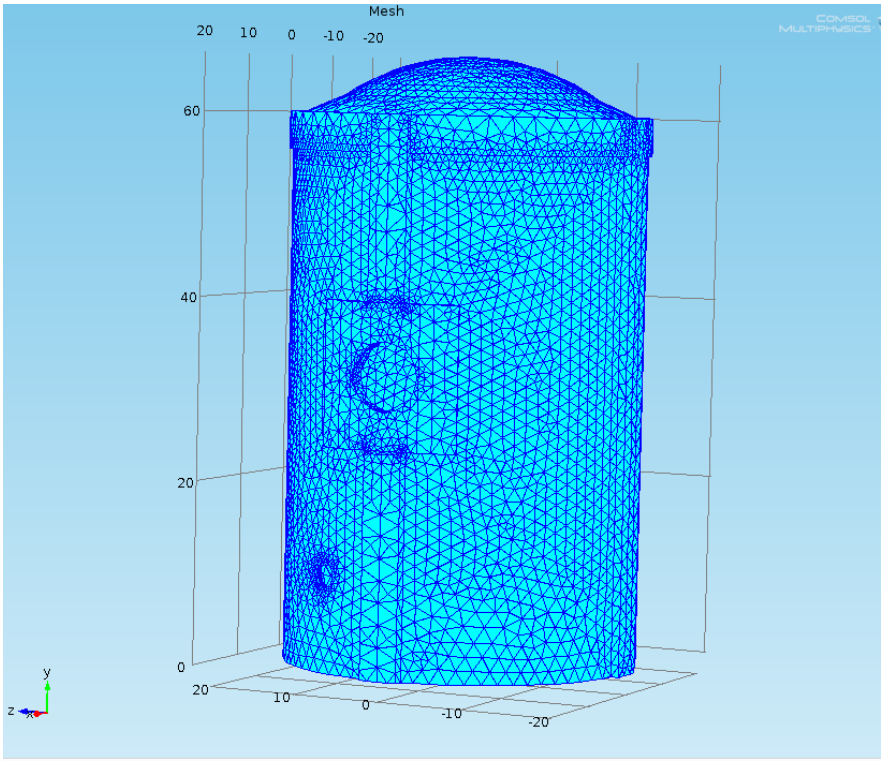

Figure 6.3 Overall quality of the applied mesh

The settings of the boundary layer mesh are shown in Figure 6.4.

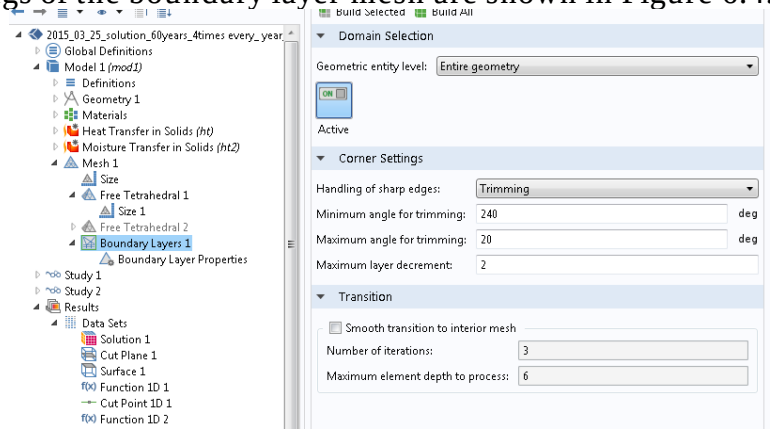

Figure 6.4 Boundary layer settings.

Furthermore, the properties of the boundary layers are shown in Figure 6.5.

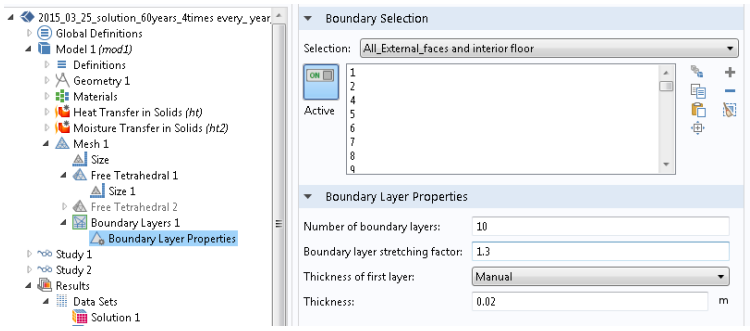

Figure 6.5 Boundary layer properties.

6.1 Limitations

The erection of a large structure as an RC is of course time consuming and would take a number of years to complete. This means that the casting is performed in different stages through the erection process. This means that the age of the concrete is not equal throughout the complete structure.

Our model starts with the assumption that the structure is erected instantly and our temperature and moisture simulation starts about 30 days after the erection.

The RC is assumed to be in operation three years after the simulation start. This means that the outdoor air temperature serve as a boundary condition on both the interior and the exterior surfaces the first three years. The effect of sun shine, cloudiness and radiation is neglected. The temperature effect of cold precipitation is also not taken into account.

When the operation of the RC starts it is assumed that the inside temperature instantly becomes stable and that there are no start up effects. This means that the temperature boundary condition is changed on the interior surface starting at three years of age.

Sheets of steel cover both the interior wall surfaces and the floor surfaces. This means that the inside RH does not affect the humidity in neither the walls nor the floor.

The concrete material is assumed not to change its properties with time.

6.2 Material

The material of the RC is modelled as a concrete described in section 3.3. The concrete material is not considered to be affected by ageing. It is considered to have reached a humidity level of 92% RH by self desiccation.

The interior surface is covered on all sides by a steel plate which is impermeable to moisture transport.

The calculations are performed with both estimated material properties according to a model and with moisture properties determined on a replica concrete.

6.3 Temperature boundary conditions

The temperature condition after erection of the RC was set to the outdoor air temperature at all surfaces but the ground foundation. At the age of three years the interior surface temperature was set to 23 °C at a level of 0 m above the foundation. This interior temperature was set to increase 0.3 °C/m in height. Figure 6.6 shows the temperature fluctuations with time at the boundary surface at a level of 0 m for the first 10 years of the simulation. The annual amplitude was set to 1 °C, after the RC was suggested to be in operation.

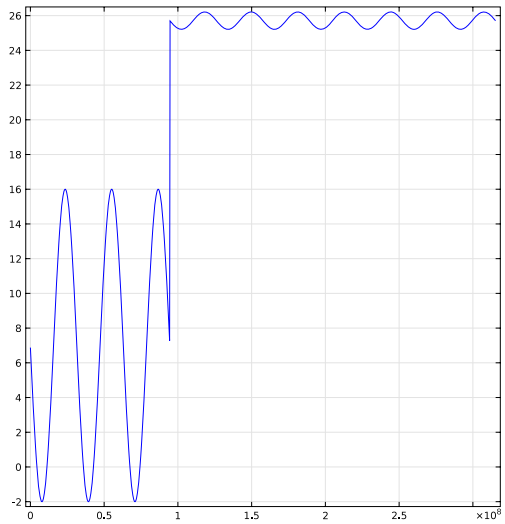

Figure 6.6 The temperature in °C at the inside boundary surface of the reactor containment at a level of 0 m above the foundation.

6.4 Method to simulate rain

The frequency of rain or precipitation at the site is approximately 15-17 days in each month throughout the year. This rain should also be included as a boundary condition in order to simulate the climatic load that is put on the RC. Two different methods were applied to simulate rain.

A first attempt was made by simulating rain with a duration of 4 hours appearing at random within a time interval of 48 hours. The actual “rain”

was simulated by increasing the relative humidity at the exterior boundary surface to 95 % RH during the four hours of rain. This attempt was not successful since the estimated time to simulate 60 years of such climatic conditions was in excess of 180 days. The maximum allowed time step had to be >1hr in order to include each rain period.

Instead a second method was suggested. The suggestion was to increase the mean relative humidity by ten percent, from 80% RH up to 90% RH. This method did not change the simulation time. That was the reason why this method was chosen to simulate the rain. However, such a high mean relative humidity is just 2% RH below the initial relative humidity, 92% RH, which in turn means that the RC wall will almost not dry at all.

7 Predicted 3D moisture distribution

The prediction of moisture distribution was conducted by using a coupled partial differential equation system regarding heat and moisture transport. The temperature simulation was run with constant heat properties unaffected by moisture content. This means that the temperature development could be simulated without simultaneously simulating the moisture transport. The simulated temperature development was used as an input to capture the suggested temperature dependency of the moisture properties.

7.1 Temperature field in general

The temperature field in the RC at the first 3 years follows the outdoor air temperature. Figure 7.1 shows the temperature field, in °C, at winter time three months after completion.

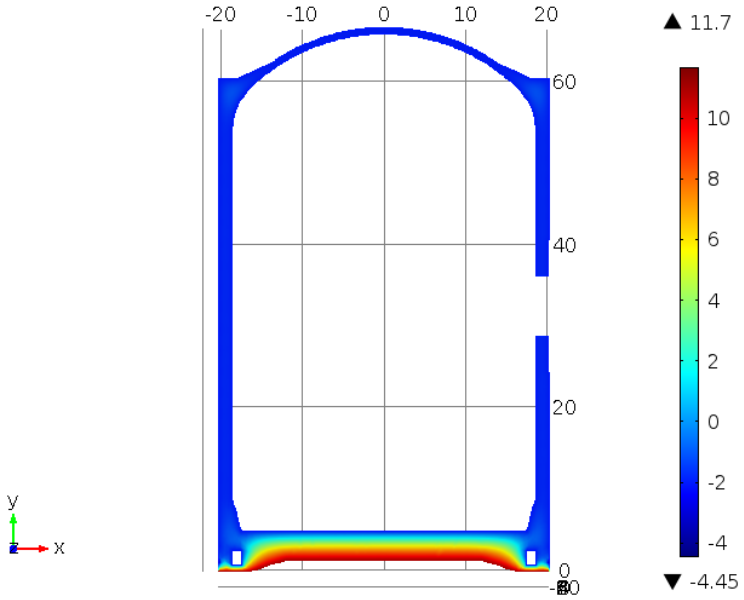

Figure 7.1 Temperature field in a vertical cross section of the reactor containment at winter time three months after completion.

Three months after completion it is assumed not to be in operation yet and therefore the RC is so cold, -4.5 °C, in general. The foundation is “heated” from the ground, which is assumed to have a temperature of 11 °C all year around.

Figure 7.2 shows the temperature field, in °C, in the RC at wintertime 59 years after completion.

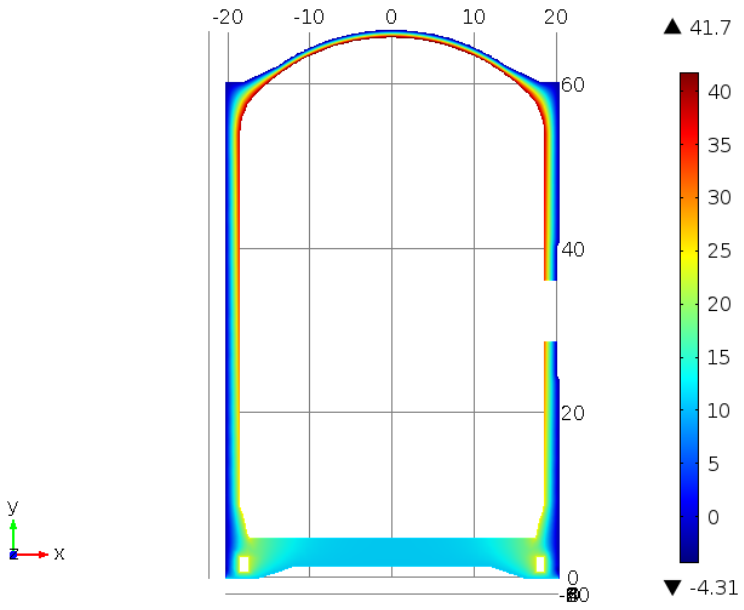

Figure 7.2 Temperature field in a vertical cross section of the reactor containment at winter time year 59.

The bar to the right shows a color legend of the temperature in °C. The highest temperature is 41.7 °C (red color) and the lowest -4.31 °C (blue color). The temperature difference between the interior and exterior concrete surface increases with the height of the RC. The largest difference is located at the centre of the concrete dome top, its magnitude is >40 °C. The smallest temperature difference is located at the foundation, <5 °C.

Unfortunately there are no measurements available of the interior temperature distribution within a real RC wall in operation. Therefore it is not possible to compare the results from the simulation with a real case.

In addition there is no recorded data of climate at the specific location that the RC is exposed to. Furthermore the exact location of the RC that is supposed to be simulated is only known on a high geographical level. It is supposed to be located near the north west coast of France, perhaps Normandie. Our attempt to model the climate is therefore very rough.

7.2 With and without rain

The results of the simulations with and without rain on the exterior wall are shown in this section. The rain was modelled as an increase of the mean RH of 10% RH according to the description of the second method, see section 6.4. The moisture properties used in this simulation were preliminary estimations performed on incomplete data from the **replica concrete**. The figures below present the RH and evaporable water content, W_e, at year 0, and from year 10, 20 up to 60 years.

7.2.1 RH distributions

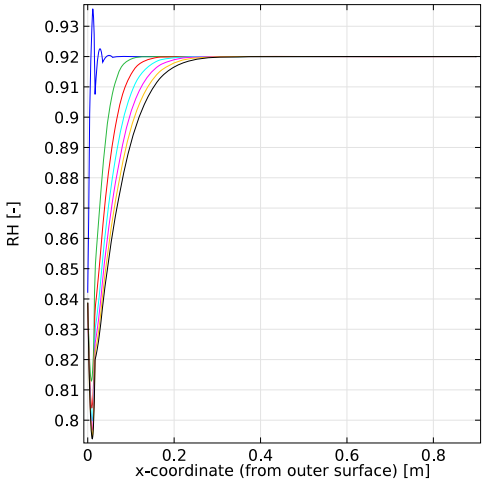

Figure 7.3 RH distribution in a RC wall 10 m above the foundation, without rain

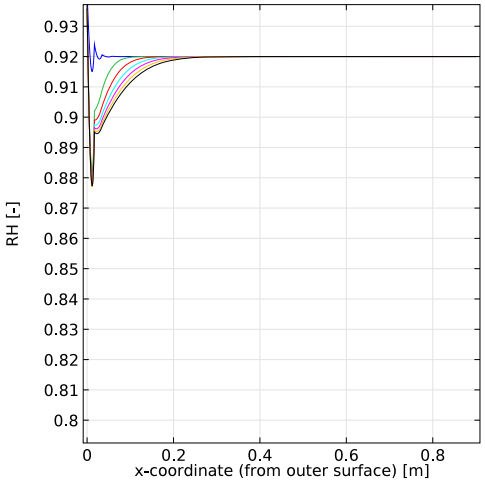

Figure 7.4 RH distribution in a RC wall 10 m above the foundation, with rain

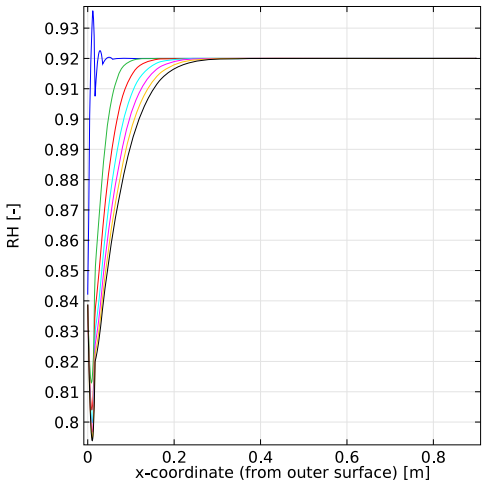

Figure 7.5 RH distribution in a RC wall 40 m above the foundation, without rain

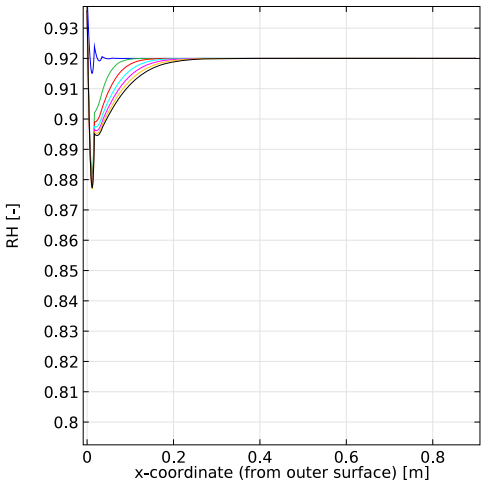

Figure 7.6 RH distribution in a RC wall 40 m above the foundation, with rain

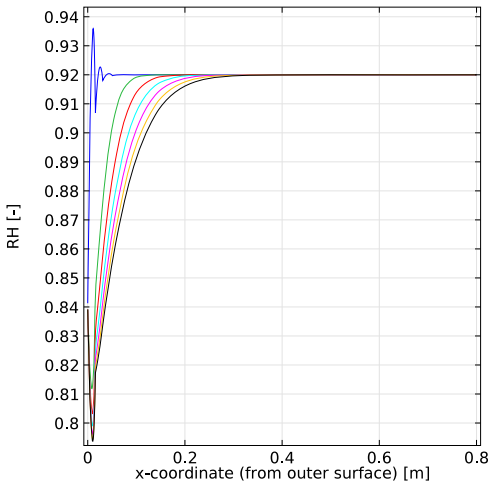

Figure 7.7 RH distribution in a RC dome top, without rain

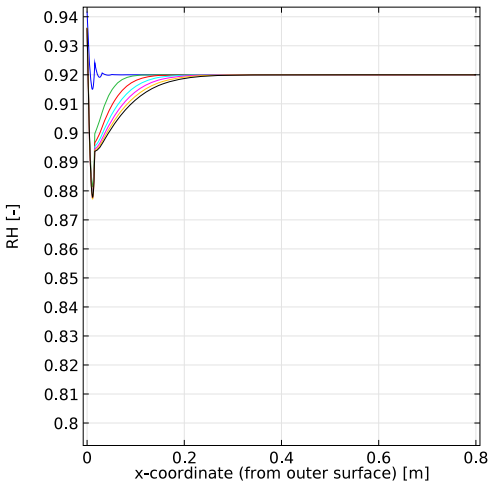

Figure 7.8 RH distribution in a RC dome top, with rain

Without a simulated rain load on the exterior surface, drying will take place in the structure. According to the simulation drying will occur to a depth of about 0.3 meters from the exterior surface.

The applied rain simulation showed that the concrete would hardly dry at all with rain. This result is not a surprise since the method to simulate rain has a profound effect of the drying RC. There will hardly be any drying at all because of the high increase of mean RH, from 80% RH without rain up

to 90% RH with rain. As the initial humidity was set to 92% RH the structure will hardly dry at all.

7.2.2 Moisture content distribution

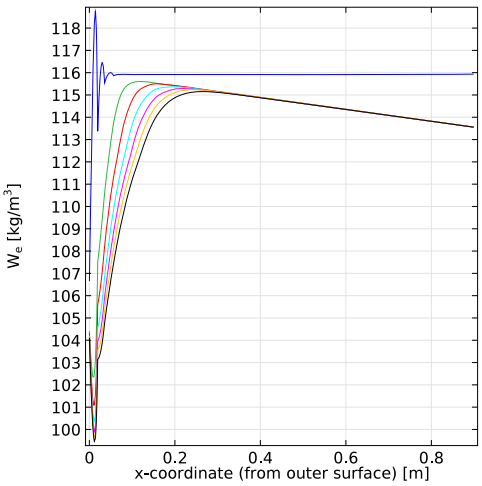

Figure 7.9 W_e distribution in a RC wall 10 m above the foundation, without rain

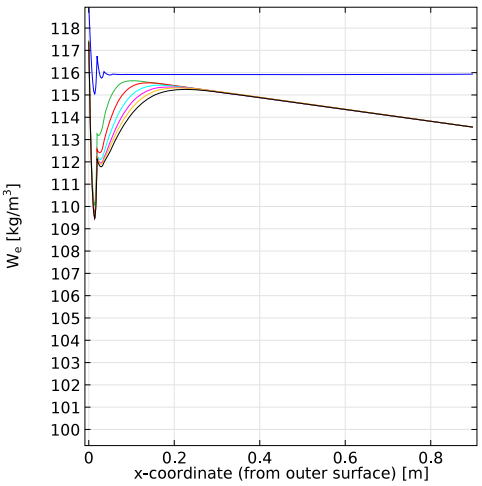

Figure 7.10 W_e Moisture distribution in a RC wall 10 m above the foundation, with rain

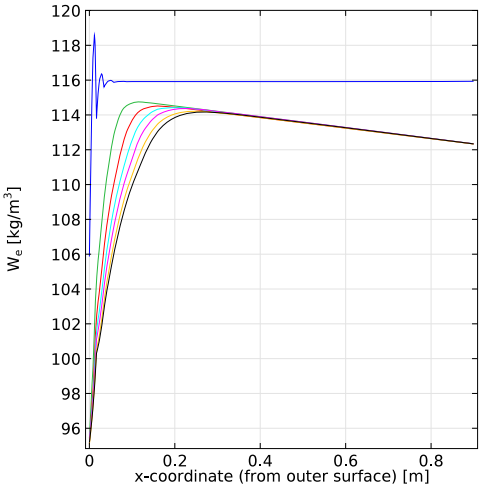

Figure 7.11 W_e distribution in a RC wall 40 m above the foundation, without rain

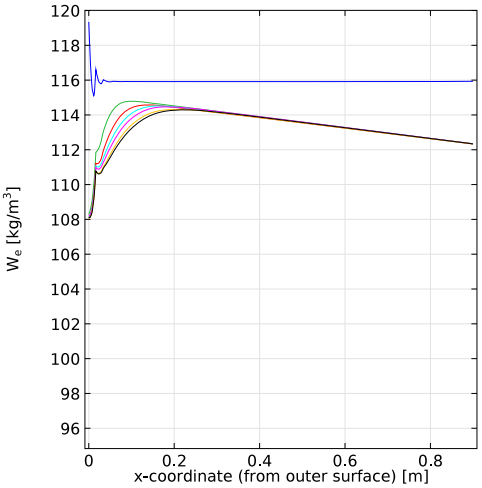

Figure 7.12 W_e distribution in a RC wall 40 m above the foundation, with rain

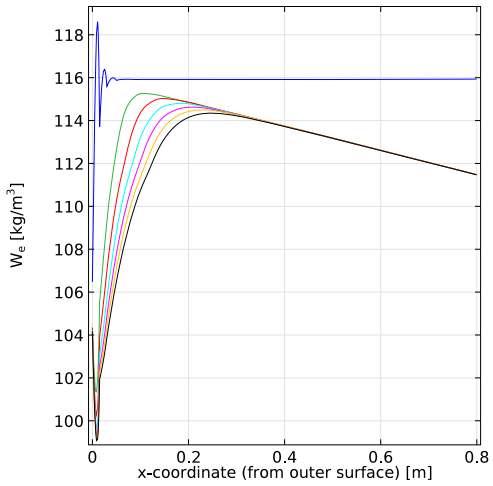

Figure 7.13 W_e distribution in a RC dome top, without rain

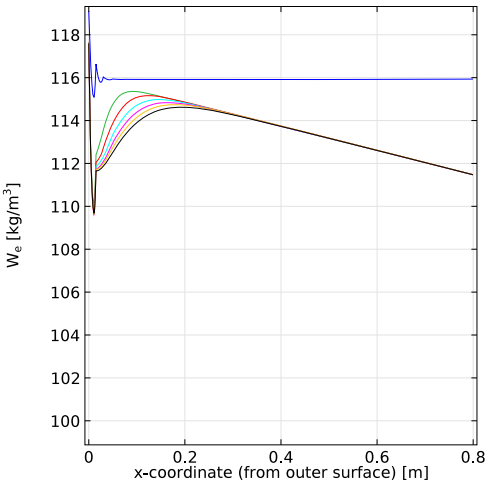

Figure 7.14 W_e distribution in a RC dome top, with rain

The results from the simulation without rain show that the moisture content decrease about 16-20 kg/m^3 at the exterior surface compared with the initial conditions. With rain this moisture content decrease is only a few kilograms, <4 kg/m^3. This may also be explained as an effect of the almost non-existing drying condition.

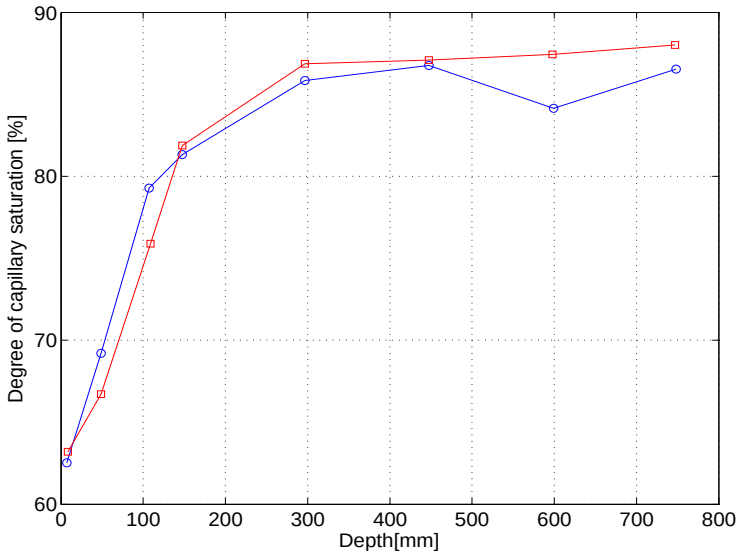

Figure 7.15 Measured moisture content profiles, as degree of capillary saturation, in a PWR containment wall after 30 years of drying under a temperature gradient [3]

The low diffusion coefficient was determined on a replica concrete that reached a higher compressive strength than did the actual concrete. Therefore it is likely that the replica concrete is denser and less permeable to moisture transport, which means that the difference in moisture

distribution between the simulation and the measurements is what could be expected. The moisture content in a real PWR has decreased substantially at the surface even if it is exposed to rain, see Figure 7.15, and this is not the case for the results from the simulation with rain. This is a rather strong indication that the suggested method to simulate rain is not realistic. The suggested increase of 10% RH at the boundary seems to be too high.

7.3 Sensitivity analysis

A sensitivity analysis was performed to investigate the impact of selecting proper moisture properties. What if the moisture capacity or the diffusion coefficient would be twice as high as suggested? How much would that affect the moisture distribution of the RC? The moisture capacity and the diffusion coefficient were multiplied by a factor of two. The case of both a double moisture capacity and a double diffusion coefficient was not tested in the same simulation. During these two simulations, the exterior humidity condition was kept constant at a level of 70% RH, but the temperature was not kept constant. The figures below presents the RH and evaporable water content at year 0, and from year 10, 20 up to 60 years.

Section 7.3.1 and section 7.3.2 show the results from a sensitivity analysis, regarding the relative humidity and moisture content, when the diffusion coefficient is twice as high as originally suggested. The results from simulations with the original diffusion coefficient, labelled with diff_coeff=1, are shown in figures to the left. The results of the simulations with a double diffusion coefficient, labelled with, diff_coeff=2 are shown in figures to the right.

Section 7.3.3 and section 7.3.4 show the results from a sensitivity analysis when the moisture capacity is twice as high as originally suggested. The results from simulations with the original moisture capacity, labelled with mc_coeff=1, are shown in figures located to the left on each page and the results of the simulations with a double moisture capacity, labelled with, diff_coeff=2 are located to the right.

7.3.1 Diffusion coefficient - Relative humidity distribution at three different locations

The relative humidity distribution is shown at a cross section through the RC wall at a level of 10 and 40 m above the foundation and it is also shown at a cross section through the centre of the dome top Figure 7.16 to Figure 7.21. The y-axis shows the relative humidity and the x-axis shows the distance from the outer surface at a cross section parallel to the radius of the RC. The legend shows the number of days since the start of the simulation, the used length of a year is 365 days, i.e. 3650 is equal to 10 years, and so on. For the location of the cross sections see Figure 6.2.

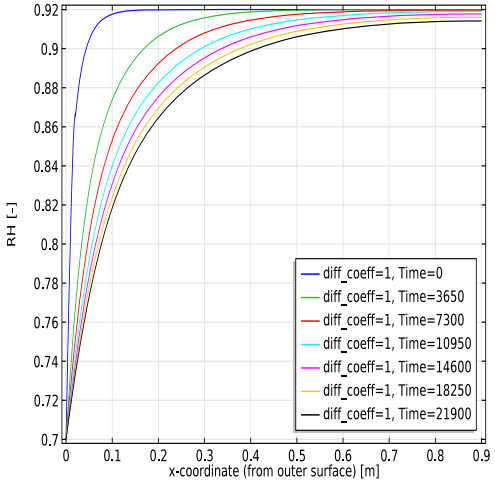

Figure 7.16 RH distribution level 10 m above foundation, diff_coeff=1.

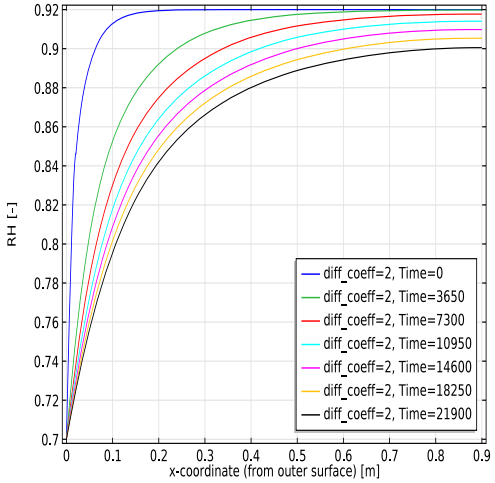

Figure 7.17 RH distribution level 10 m above foundation, diff_coeff=2

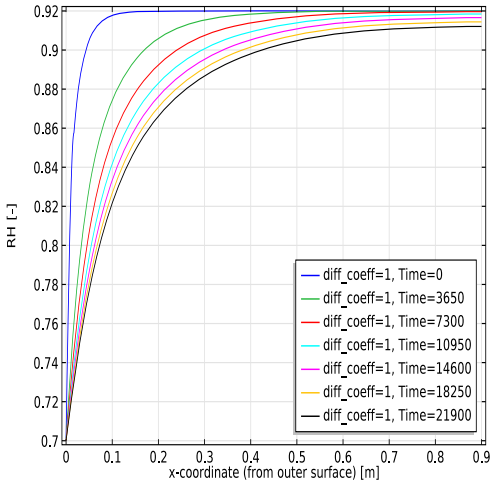

Figure 7.18 RH distribution level 40 m above foundation, diff_coeff=1

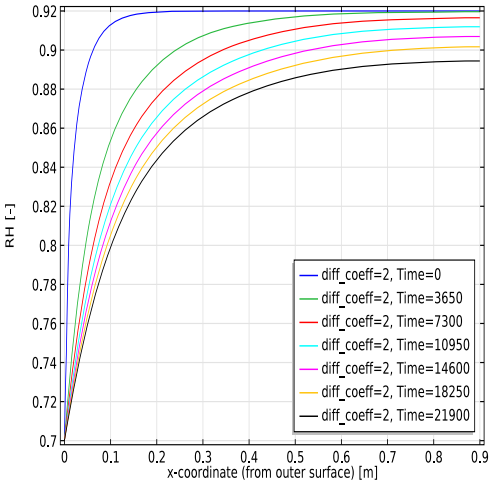

Figure 7.19 RH distribution level 40 m above foundation, diff_coeff=2.

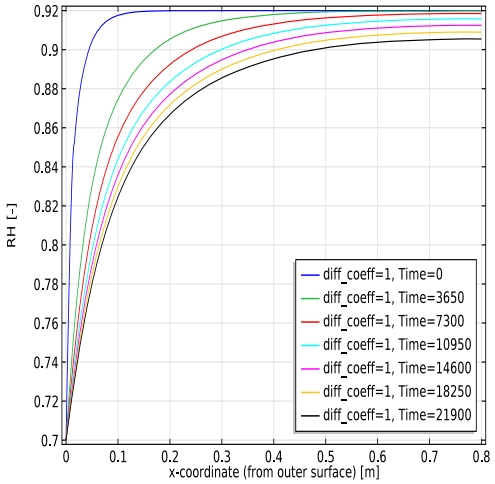

Figure 7.20 RH distribution at the dome top, diff_coeff=1.

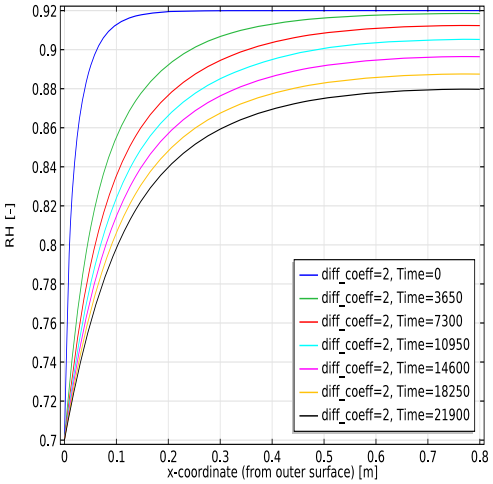

Figure 7.21 RH distribution at the dome top, diff_coeff=2

The result from this simulation is rather straight forward. An increase in diffusion coefficient gives a higher degree of drying. In addition, a larger the temperature gradient gives a faster drying rate, hence decreasing the moisture content more than if the structure would be subjected to a smaller temperature gradient. As the temperature inside the structure is always higher than the inside, the drying rate increases. This increase is a direct effect of the moisture transport model that suggests that the diffusion coefficient increases with an increase of temperature. In addition, the temperature gradient is also higher at the dome top compared with the foundation. This is why the drying rate is faster at the dome top that is exposed to a larger temperature gradient than parts closer

to the foundation at a lower elevation. All of the results from this simulation are plausible. It is not possible to say which is the most correct, without performing a proper measurement. A measurement of the RH distribution in a structure may make one solution more probable than another.

7.3.2 Diffusion coefficient – Moisture content distribution at three different locations

In this section the moisture content distribution is shown at a cross section through the RC wall at a level of 10 and 40 m above the foundation and it is also shown at a cross section through the centre of the dome top, see Figure 7.22 to Figure 7.25 and Figure 7.27to Figure 7.28. For the location of the cross section Figure 6.2

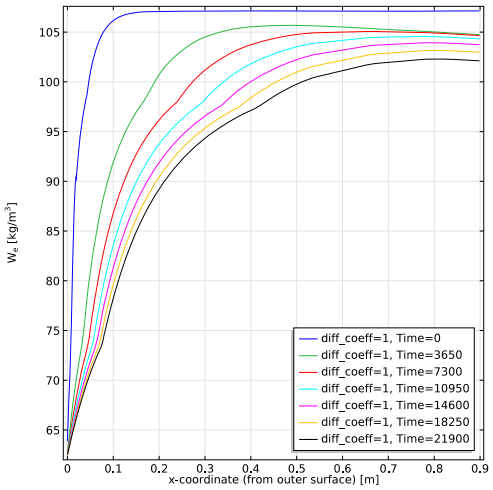

Figure 7.22 We distribution at level 10 m above the foundation, time represents the number of days, is noted in days, diff_coeff=1

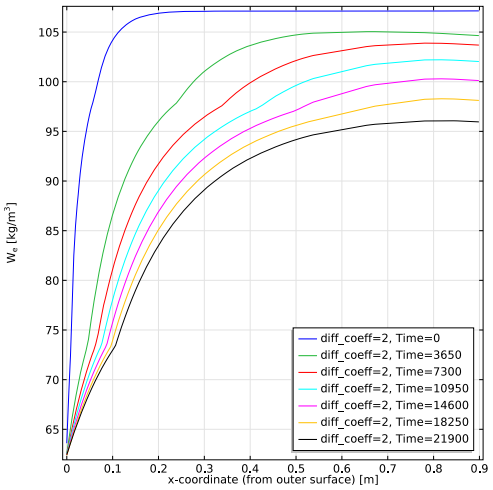

Figure 7.23 We distribution at level 10 m above the foundation, diff_coeff=2

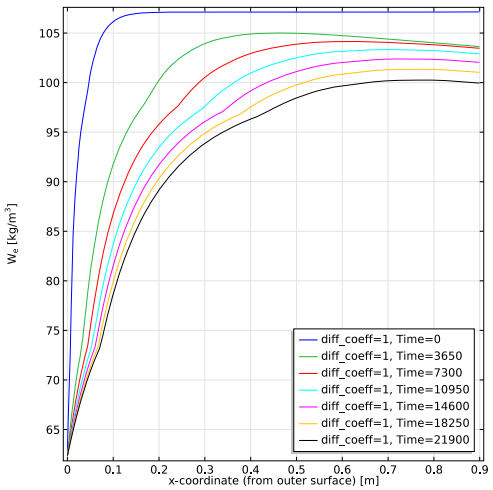

Figure 7.24 W_e distribution at level 40 m above the foundation, diff_coeff=1

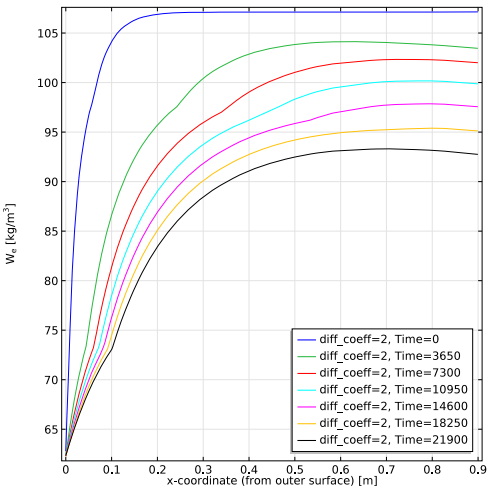

Figure 7.25 W_e distribution at level 40 m above the foundation, diff_coeff=2

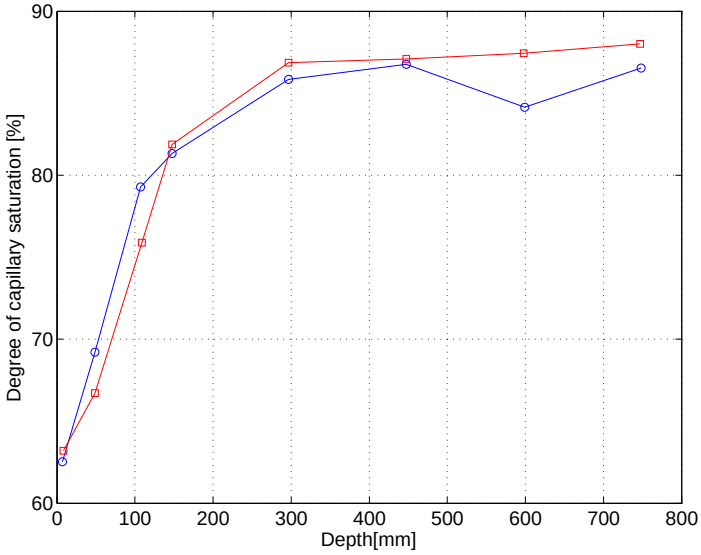

Figure 7.26 Measured moisture content profiles, as degree of capillary saturation, in a PWR containment wall after 30 years of drying under a temperature gradient[3].

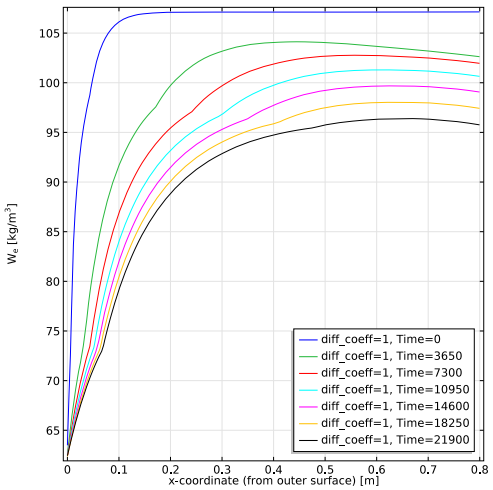

Figure 7.27 W_e distribution at the dome, diff_coeff=1.

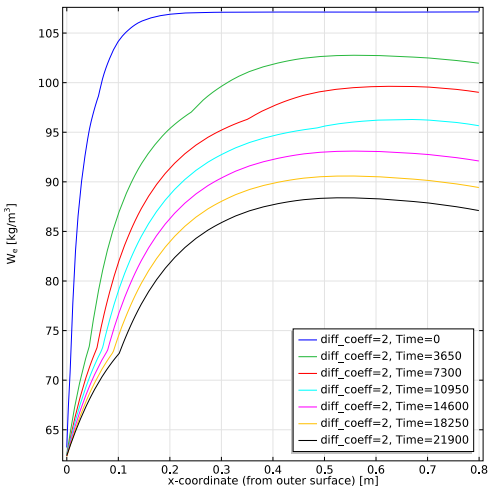

Figure 7.28 W_e distribution at the dome, diff_coeff=2.

The distributions of moisture content show that the structure has dried significantly. The decrease in moisture content is more pronounced if the diffusion coefficient is higher, which is clearly shown by comparing e.g. Figure 7.27 with Figure 7.28. The difference in temperature gradient affects both the diffusion coefficient and the desorption isotherm. The diffusion coefficient increases but the materials ability to contain moisture decreases. It is therefore reasonable that the moisture content decreases more when the temperature gradient increases.

7.3.3 Moisture capacity - Relative humidity distribution at three different locations

The relative humidity distribution is shown at a cross section through the RC wall at a level of 10 and 40 m above the foundation and it is also shown at a cross section through the centre of the dome top, see Figure 6.2. The y-axis shows the relative humidity and the x-axis shows the distance from the outer surface at a cross section parallel to the radius of the RC. The legend shows the number of days since the start of the simulation, the used length of a year is 365 days. , i.e. 3650 is equal to 10 years, and so on. Two moisture capacities were used, the original, labelled with mc_coeff=1 was derived from the modelled desorption isotherm, see Figure 3.3. The results with a twice as high moisture capacity are shown to the right and are labelled mc_coeff=2.

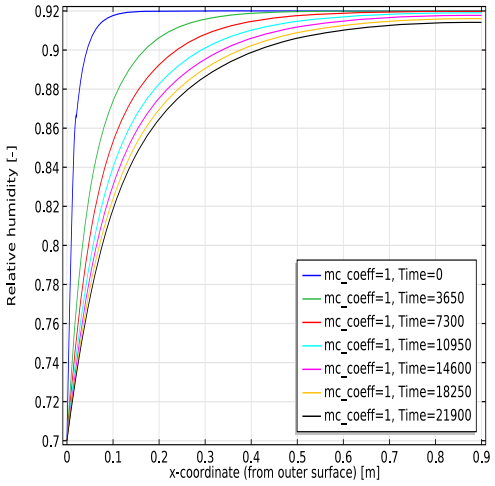

Figure 7.29 RH distribution at level 10 m above foundation, mc_coeff=1

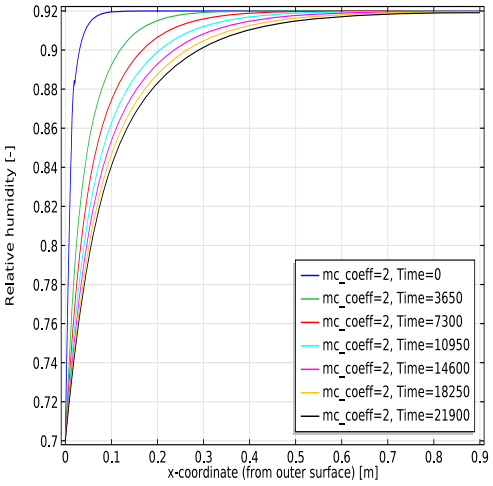

Figure 7.30 RH distribution at level 10 m above foundation, mc_coeff=2

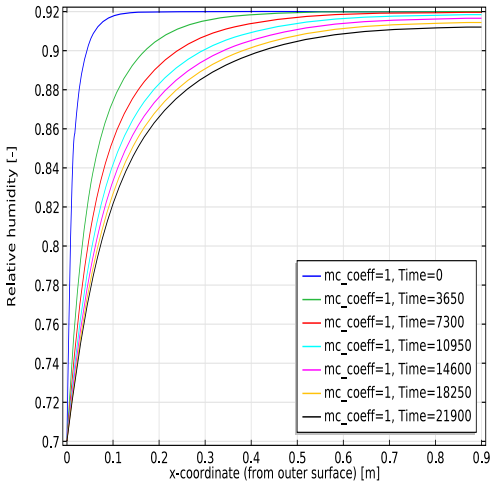

Figure 7.31 RH distribution at level 40 m above foundation, mc_coeff=1

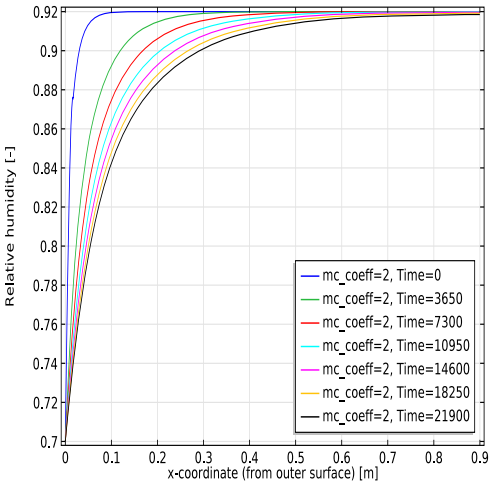

Figure 7.32 RH distribution at level 40 m above foundation, mc_coeff=2

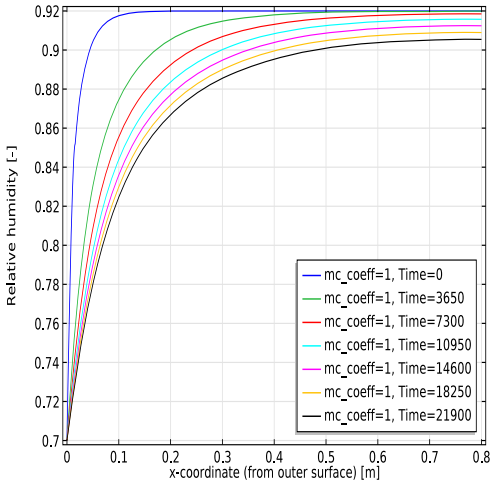

Figure 7.33 RH distribution at centre of dome top, mc_coeff=1

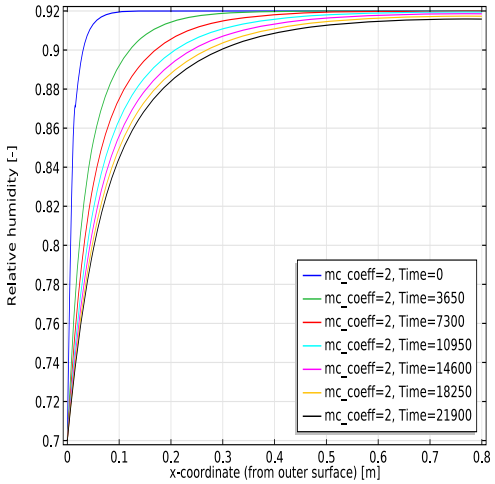

Figure 7.34 RH distribution at centre of dome top, mc_coeff=2

The result from the simulation shows that the RH increases if the moisture capacity is higher. Such a result is not as straight forward as was the result of the diffusion coefficient analysis. One must bear in mind what parameter that determines the moisture flow; and it is the diffusion coefficient. When the diffusion coefficient is unchanged the moisture flow does not change, given an equal drying potential. The moisture flow determines the decrease in moisture content. If the reduction of moisture content is equal in two materials with different moisture capacity; then the decrease in RH is larger in the material exhibiting a smaller moisture capacity. It is not possible to determine which of the above RH distributions that is more accurate or realistic than the other. Such a question may be possible to answer by performing RH measurements on a concrete structure exposed to a similar climate condition.

7.3.4 Moisture capacity – Moisture content distribution at three different locations

The moisture content at a cross section through the RC wall is shown at a level of 10 and 40 m above the foundation. It is also shown at a cross section through the centre of the dome top. The y-axis shows the moisture content and the x-axis shows the distance from the outer surface at a cross section perpendicular to the surface of the RC. Two different moisture capacities are used, the first which is derived from the modelled desorption isotherm, see Figure 3.3, multiplied by a coefficient of 1, mc_coeff=1. The second moisture capacity is derived from the same desorption isotherm and multiplied with a coefficient of 2, mc_coeff=2.

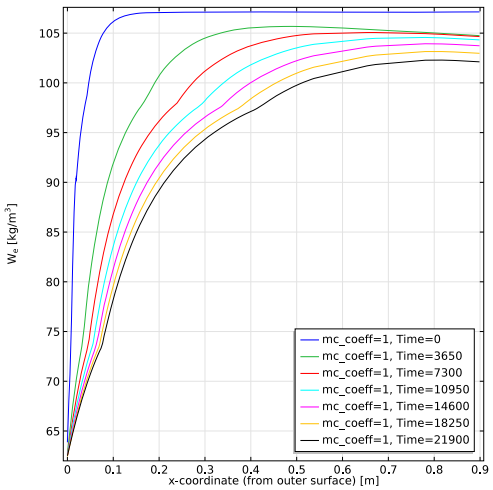

Figure 7.35 We distribution at level 10 m above foundation, mc_coeff=1

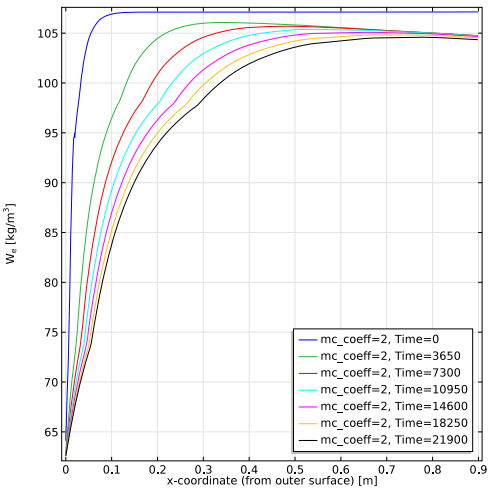

Figure 7.36 We distribution at level 10 m above foundation, mc_coeff=2

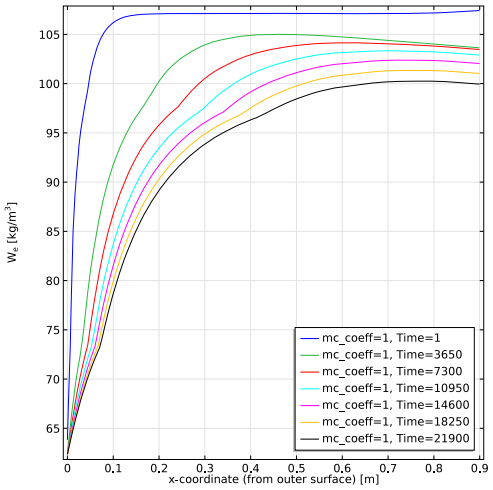

Figure 7.37 We distribution at level 40 m above foundation, mc_coeff=1

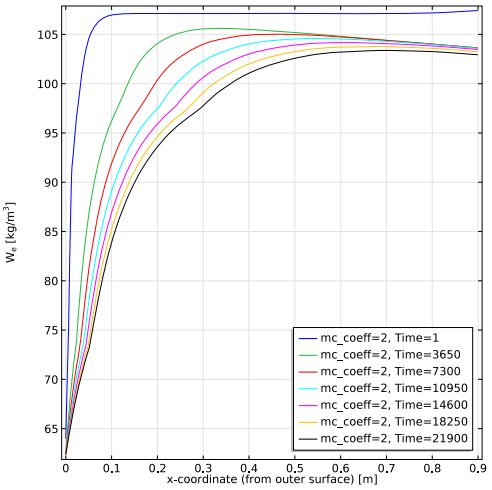

Figure 7.38 We distribution at level 40 m above foundation, mc_coeff=2

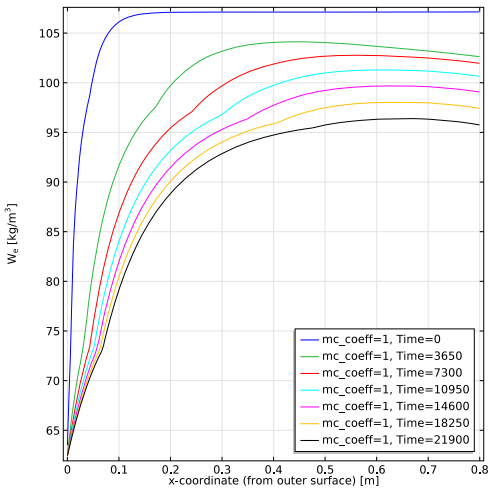

Figure 7.39 We distribution at centre of dome top, mc_coeff=1

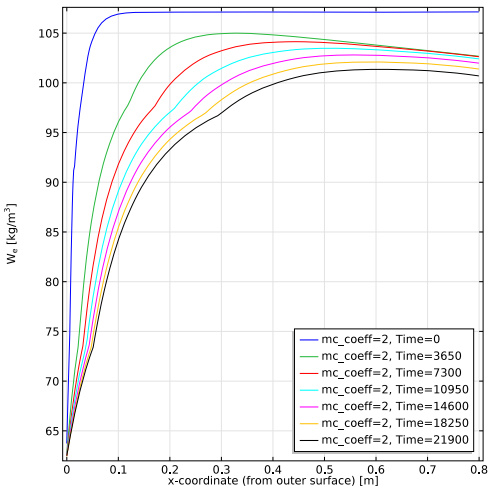

Figure 7.40 We distribution at centre of dome top, mc_coeff=2

An increase of the moisture capacity has a different impact of the moisture content distribution compared with the impact of an increase of the diffusion coefficient. The relative humidity becomes higher at the steel liner when the moisture capacity is higher. This means that the drying decreases if the moisture capacity is larger than expected.

7.4 Moisture parameters from the replica concrete

The moisture parameters determined in the experimental works of this project were applied in a simulation with a constant RH of 80% RH, on the external surface of the RC. The temperature conditions in this simulation were equal to the temperature filed in general.

The distribution of RH is shown at cross sections through the RC wall at a level of 10 and 40 m above the foundation, see Figure 7.41 and Figure 7.42. It is also shown at a cross section through the centre of the dome top, see Figure 7.43.

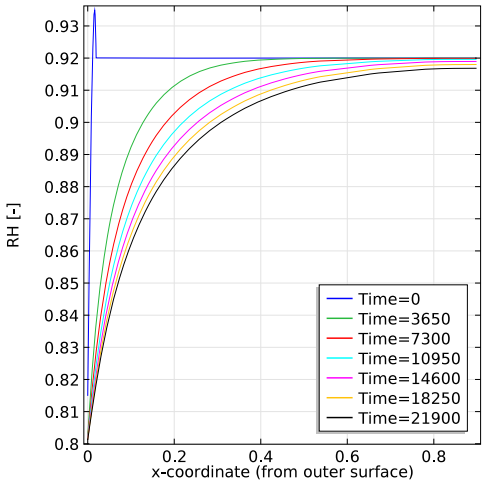

Figure 7.41 RH distribution at level 10 m above foundation

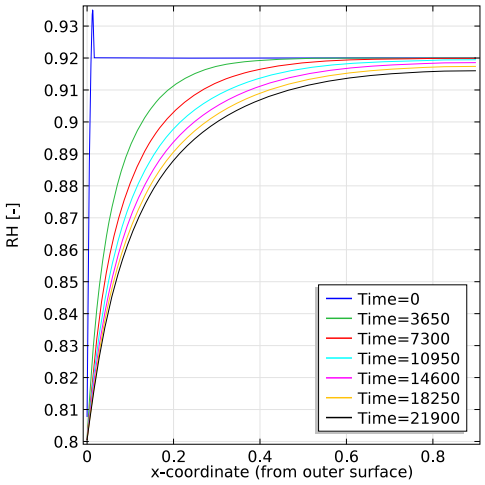

Figure 7.42 RH distribution at level 40 m above foundation

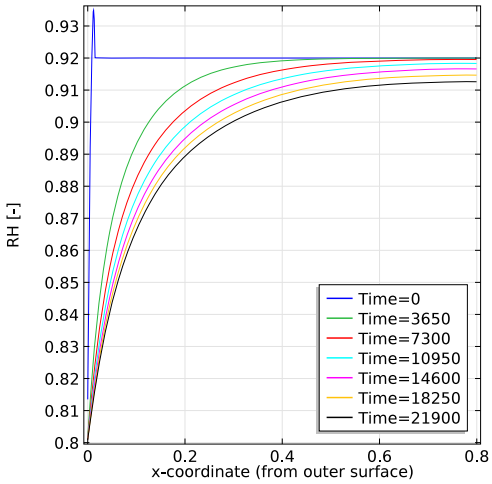

Figure 7.43 RH distribution at centre of dome top

The results from the simulations clearly show that the higher temperature gradient the larger decrease in RH, i.e. a higher degree of drying is

achieved. This is a direct consequence of the applied temperature dependency of the diffusion coefficient, the higher the temperature the larger the diffusion coefficient. In other words when the boundary conditions in terms of RH are constant; moisture transport increases with an increasing temperature gradient. The RH at the steel plate located at x-coordinate 0.9 m decreases the most at the dome top; which is also subjected to the largest temperature gradient.

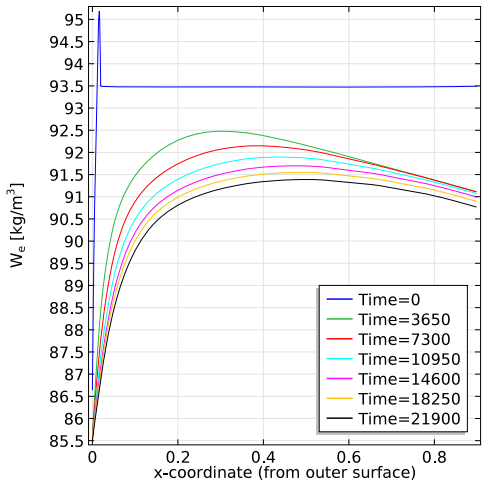

Figure 7.44 W_e distribution at level 10 m above above foundation

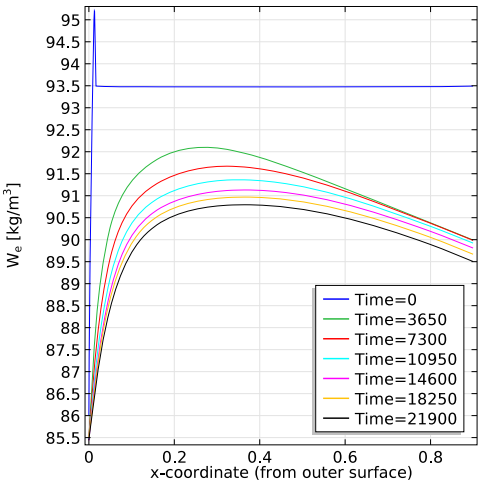

Figure 7.45 W_e distribution at level 40 m above above foundation

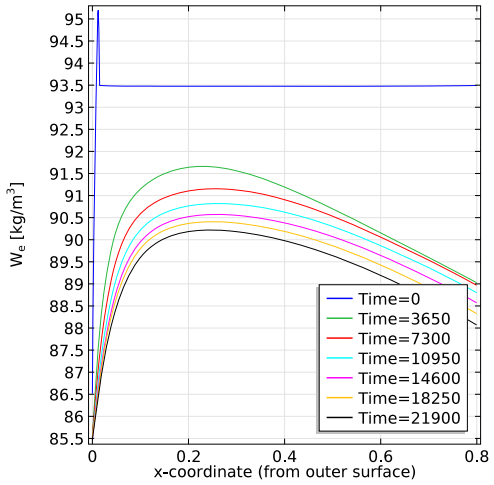

Figure 7.46 W_e distribution at centre of dome top

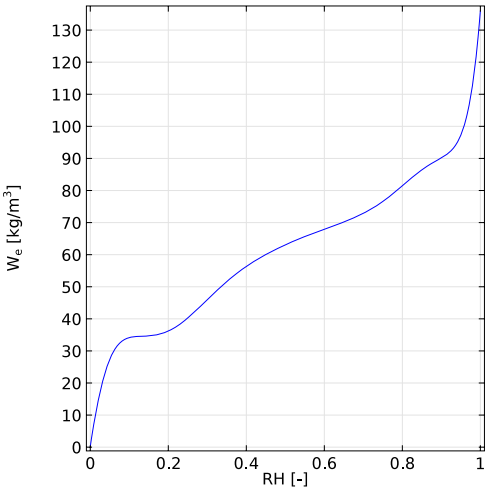

Figure 7.47 Sorption isotherm assessed from the replica concrete shown at a temperature of 20 °C

The results from the simulations clearly show that reduction in moisture content is rather low. The lower moisture content at the steel plate at x-coordinate 0,8 m, cf Figure 7.46, is an effect of drying but also an effect of the desorption isotherms temperature dependency. This is a direct consequence form the small moisture capacity that the replica concrete exhibits in the RH range of the simulation from 92 % RH down to 80% RH. The moisture capacity of the replica concrete is repeated here for convenience, see Figure 7.47.

7.5 The current moisture and temperature conditions after 30 years in operation

The best agreement between the results from the simulations performed and the measurements on a real RC in Sweden was found when the rain load was neglected and the moisture properties was roughly modelled by using Hedenblads results [2]. This means that results from the sensitivity analysis simulation regarding the impact of the diffusion coefficient, see Figure 7.48 -Figure 7.49, matched the measured moisture distribution, see Figure 7.51, on a qualitative basis. The temperature distributions through a RC wall is shown in Figure 7.50

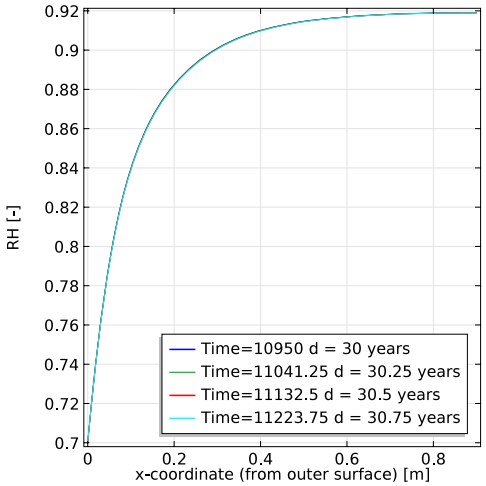

Figure 7.48 RH distributions at a level of 10 meter above the foundation level

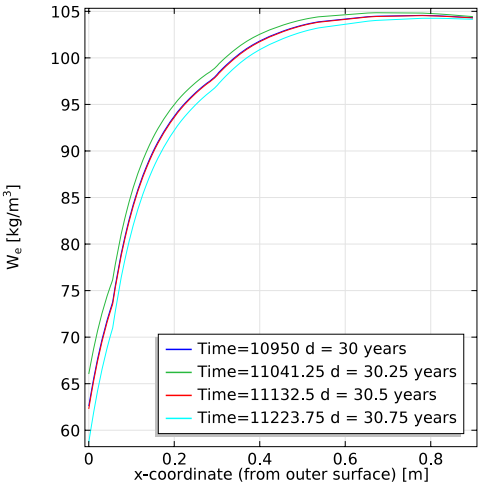

Figure 7.49 Moisture content distributions at a level of 10 meter above the foundation level

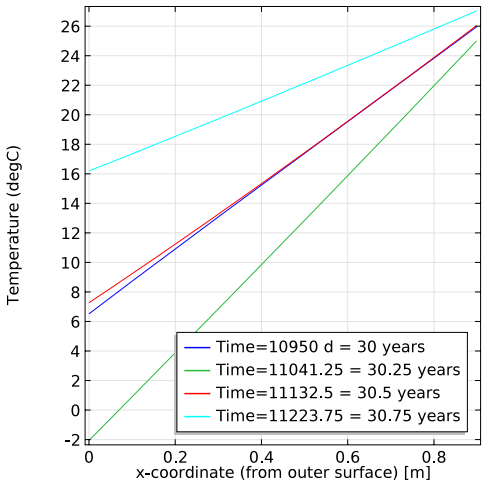

Figure 7.50 Temperature distributions at a level of 10 meter above the foundation level

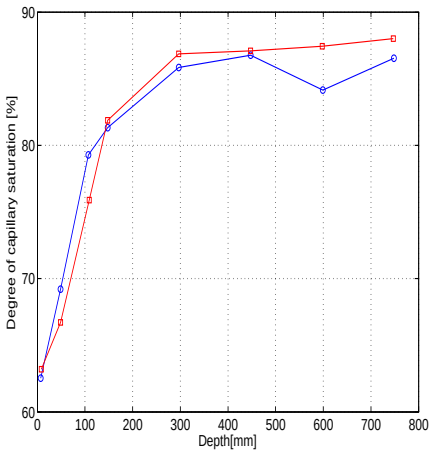

Figure 7.51 Measured moisture content distributions, as degree of capillary saturation, in a PWR containment wall after 30 years of drying under a temperature gradient [3]

8 Additional remarks

There were a few obstacles that needed to be cleared to make it possible to exchange data to and from project G3 to G4.

G3 and G4 used two different computer soft wares, Abaqus and Comsol multiphysics. This complicated the procedure of data exchange, i.e. moisture content and temperature, from G4 to G3. The data from the simulations performed in G4 was exported from Comsol as a number of txt-files, with information on the x-, y-, z-coordinates with corresponding mean moisture content and mean temperature. The mean values were originated from the results of four moments in time during one year, one for each season. This txt-file with the mean values was imported and transferred to a mat-file (Matlab) by G4. These m-files were later sent to G3. The data was then treated by G3 and imported into Abaqus using a certain algorithm because of different mesh configurations.

The simulations performed by G3 was for instance, to determine shrinkage, creep and the affect that has on the pre-stressed reinforcement and in order to do that the simulation results of G4 was used as an input. The number of freedoms on these simulations were larger for G3 than G4.

The simulations by G3 and G4 were performed by using two different meshes. The reason for that is that the hygro-thermal simulation has a need of a denser mesh at the surfaces in order to achieve a reasonably realistic moisture distribution through a cross section. As there is only two degrees of freedom, RH and temperature, in each mesh node there is a possibility to perform a number of simulations even if there is a dense mesh near the surfaces. The number of the degrees of freedom of the mesh, dof, was about 365000. Due to the assumption that the thermal properties of the concrete are not influenced by the moisture content, the heat transfer simulation and and the moisture simulation could be performed separately, starting with the heat transfer simulations.

The simplifications of the modelling were made in order to make it possible to simulate the moisture conditions of an RC through 60 years of operation. It was not possible to include the effect of daily variations of heat transfer of solar radiation, cloudiness, a detailed model to capture the exposure to rain.

The resulting relative humidity, RH, distribution at time zero generated from the sensitivity analysis does not correctly represent the near surface RH distribution. The RH distribution in the concrete structure at time zero must regardless to the air RH (which in this analysis has been equated to 70 %) be uniform and equal to the initial RH which is condition 92%. As the RH is not uniform at time zero the moisture content distribution is neither uniform, since it correlates with the sorption isotherm. One reason for this result, is that the simulation used a simplification of the boundary

condition, which was set to a constant RH. Another reason for this poor result is the mesh, which is also not as dense as it should be to capture a probable moisture distribution at time zero. The boundary condition was set as a relative humidity condition and, for instance the, surface resistance of the moisture transport was neglected.

Simulation results generated from the model after time zero are more probable since the effect of the simplified description of the boundary conditions decreases with time. This means that the moisture content distributions from year 1 and forward, are more probable also near the surface.

9 Conclusion

A model of moisture and heat transfer was developed to simulate the moisture and heat conditions in a RC in a PWR. This model takes into account the temperature dependency of the moisture properties. It is also possible to include the heat properties dependency of the materials moisture condition; this was however not tested in this project.

The simulated moisture distributions on the French concrete RC were compared with results from measurement performed on a Swedish concrete RC [3]. Please note that these measurements were not performed in this project. The simulation in this project and the moisture distribution determined on the Swedish concrete RC were found to qualitatively correspond to each other. Since proper material data from the actual materials were not obtainable and no measurements were allowed on the RC there is no possibility to compare the simulation quantitatively.

A rough rain analysis showed that the results from the employed model did not correspond to the measurements from a real RC wall. The applied rain exposure model seems to exaggerate the impact on the moisture content distribution.

The diffusion coefficient is an important parameter that has a significant impact on the moisture conditions in the RC wall. Both the RH- and the moisture content decrease significantly if the diffusion coefficient is multiplied by a factor of two.

In contrast, a twice as large moisture capacity does not have a significant on the moisture content. However, the drying of the RC was more pronounced when the moisture capacity was lower.

This research came to the conclusion that it is difficult to make a replica concrete of the concrete actually used in the RC, and to determine moisture properties to be used in the simulations. One obvious reason for this, is that it is difficult to find the materials used in the original concrete mixture. Based on this conclusion, it would be a good idea to cast extra samples of the concrete used in the RC. These extra samples could be used in the future to determine different material properties needed to perform an estimation of the remaining service life.

10 References

1. Nilsson, L.O. and P. Johansson, *Förändringsprocesser i reaktorinneslutningar Betongväggarnas klimatförhållanden och uttorkning*. 2009.
2. Hedenblad, G., *Moisture permeability of mature concrete, cement mortar and cement paste*. 1993, Div. of Building Materials, Lund University.
3. Oxfall, M., P. Johansson, and M. Hassanzadeh. *Moisture profiles in concrete walls of a nuclear reactor containmen after 30 years of operation*. in *Nordic Concrete Research - Proceedings of XXII Nordic Concrete Symposium*. 2014. Reykjavik, Iceland: Norsk Betongforening.
4. Åhs, M., et al. *A model to predict moisture conditions in concrete reactor containments*. in *Fontevraud 8 – SFEN International Symposium - September 15-18*. 2014. Avignon.
5. Nilsson, L.O. and P. Johansson, *Climatic conditions at the surfaces of concrete containments – examples for two BWR and PWR reactors*. Transactions, 2007. **SMiRT 19**(Paper # DH01/2): p. 1-8.
6. Nilsson, L.O., *Hygroscopic moisture in concrete - Drying, measurements & related material properties*. 1980, Lund University, Lund Institute of Technology.
7. Poyet, S., *Experimental investigation of the effect of temperature on the first desorption isotherm of concrete*. Cement and Concrete Research, 2009. **39**(11): p. 1052-1059.
8. Poyet, S. and S. Charles, *Temperature dependence of the sorption isotherms of cement-based materials: Heat of sorption and Clausius-Clapeyron formula*. Cement and Concrete Research, 2009. **39**(11): p. 1060-1067.
9. Mainguy, M., O. Coussy, and V. Baroghel-Bouny, *Role of Air Pressure in Drying of Weakly Permeable Materials*. Journal of Engineering Mechanics, 2001. **127**(6): p. 582-592.
10. Baroghel-Bouny, V., et al., *Characterization and identification of equilibrium and transfer moisture properties for ordinary and high-performance cementitious materials*. Cement and Concrete Research, 1999. **29**: p. 1225-1238.
11. Poyet, S., *Determination of the intrinsic permeability to water of cementitious materials: Influence of the water retention curve*. Cement and Concrete Composites, 2013. **35**(1): p. 127-135.
12. Poyet, S., et al., *Assessment of the unsaturated water transport properties of an old concrete: Determination of the pore-interaction factor*. Cement and Concrete Research, 2011. **41**(10): p. 1015-1023.

13. van Genuchten, M.T., *A Closed-form Equation for Predicting the Hydraulic Conductivity of Unsaturated Soils1.* Soil Sci. Soc. Am. J., 1980. **44**(5): p. 892-898.
14. Mualem, Y., *A new model for predicting the hydraulic conductivity of unsaturated porous media.* Water resources research, 1976. **12**(3): p. 513-522.